[redacted]

UNCLASSIFIED

WT-2057-SA

This document consists of 49 pages.

No. 140 of 235 copies, Series A.

Operation

DOMINIC

HAZARDS EVALUATION UNIT REPORT

BLAST PREDICTIONS AT CHRISTMAS ISLAND,

Sanitized Version

Jack W. Reed and Hugh W. Church

Sandia Laboratory
Albuquerque, New Mexico

Issuance Date: October 25, 1963

DISTRIBUTION STATEMENT A
Approved for public release;
Distribution Unlimited

19980716 001

[redacted]

[redacted]

[redacted]

DECLASSIFIED WITH DELETIONS
DSWA OPSSI NTPR REVIEW
DISTRIBUTION STATEMENT A
APPLIES TO THIS VERSION ONLY.
[redacted] DATE 6/12/98
COORDINATED WITH
C. DEMOS & F. HALAZ (DOE-ALO)

[redacted]

68-888,866

UNCLASSIFIED

When no longer required, this document may be destroyed in accordance with applicable security regulations.

DO NOT RETURN THIS DOCUMENT

USAEC Division of Technical Information Extension, Oak Ridge, Tennessee

WT-2057

Operation Dominic

Hazards Evaluation Unit Report

BLAST PREDICTIONS AT CHRISTMAS ISLAND

By

Jack W. Reed

and

Hugh W. Church

Sandia Laboratory
Albuquerque, New Mexico
August 1963

[redacted]

[redacted]

[redacted]

ABSTRACT

Blast pressures from the Dominic Christmas Island tests were recorded at four stations at varying distances of from 10 to 40 miles as a support activity for blast safety prediction.

It was found that atmospheric refraction often influenced blast pressures to a considerable degree at these long ranges. Under usual conditions adequate predictions are made with standard pressure-distance curves scaled for yield and height of burst in situations where refracted sound rays are calculated to strike the gage location. In situations where sound rays are calculated to bend away from ground, a diffracted wave strikes the gage, and in this diffraction zone overpressure decays in proportion to distance squared.

In the few-tenths-psi range of overpressures, many records showed strong initial pressure spikes which on occasion reached to double the solid pulse pressure. These spikes are real, last several milliseconds, and appear to be strongest when sound velocity increases with height above ground. Such spikes may be significant in determination of causes of light damage; they have not, however, been satisfactorily explained.

CONTENTS

ILLUSTRATIONS

TABLES

BLAST PREDICTIONS AT CHRISTMAS ISLAND

1 INTRODUCTION

Twenty-four air-burst bomb tests were carried out near Christmas Island during Operation Dominic. These tests were conducted at altitudes between 2500 and 15,000 feet above the surface of the ocean and from 10 to 30 miles distance from island instrumentation stations. Test yields ranged up to 7 megatons. Primary concerns for blast predictions were for personnel safety, both in the main Joint Task Force (JTF-8) camp and in London Village where between 400 and 500 Gilbertese workers lived. Blast prediction was also necessary to assure that aircraft parked at the airstrip would not be damaged.

At forward instrumentation stations, Site A and Site M (see Fig. 1), blast intensity was restricted to allow for continuous test operations. Early in the operation an upper limit of 0.7-psi blast overpressure was believed necessary at these forward instrument sites. Higher pressures were expected to damage trailers to an extent which might slow operations.

Most tests were conducted at heights of burst where blast pressures were considerably enhanced by Mach stem formation. Previous large weapons tests at Eniwetok and Bikini were mostly surface bursts, and there had been little experience with over-water bursts at tactical altitudes. Height-of-burst "knee" effects[1] were expected to be preserved in over-water testing, but there was no certainty that quantitative adjustments would not be necessary. Furthermore, the relatively fast decay of overpressure with distance which was found in PPG tests,[2] as compared to theoretical homogeneous atmosphere decay, was believed to be associated with upward refraction of sound and shock rays in the strong temperature-height gradient of tropical oceanic areas. As a result, pressure pulses below about 3 psi recorded at ground level from earlier testing were largely propagated by diffraction. If this were truly the cause of reduced pressure-distance curves from megaton tests, similarly reduced pressures might not be equally appropriate for bursts at the height of the Dominic Christmas Island tests.

Early predictions for these tests established target locations remote enough to hold damage below an acceptable limit. First estimates, however, were based on limited observations of Ivy King[3] and Redwing Cherokee shots.[4] In view of these uncertainties in blast prediction, a small measurement program attempted a check on height-of-burst (HOB) effects for these over-water explosions.

2 INSTRUMENTATION

Pressure gage recordings were made at the Joint Operations Center (JOC) and London Village (LON), mapped in Fig. 1. At both Site A and Site M two Wiancko pressure transducers were mounted about four feet above ground, side-on to bursts. One 1/2-psi and one 1-psi gage were used at each station. Installation was made several hundred feet from the nearest camp building or trailer, and over regular, flat terrain of piled coral rocks. No significant irregularities from blast-thermal interactions were expected.

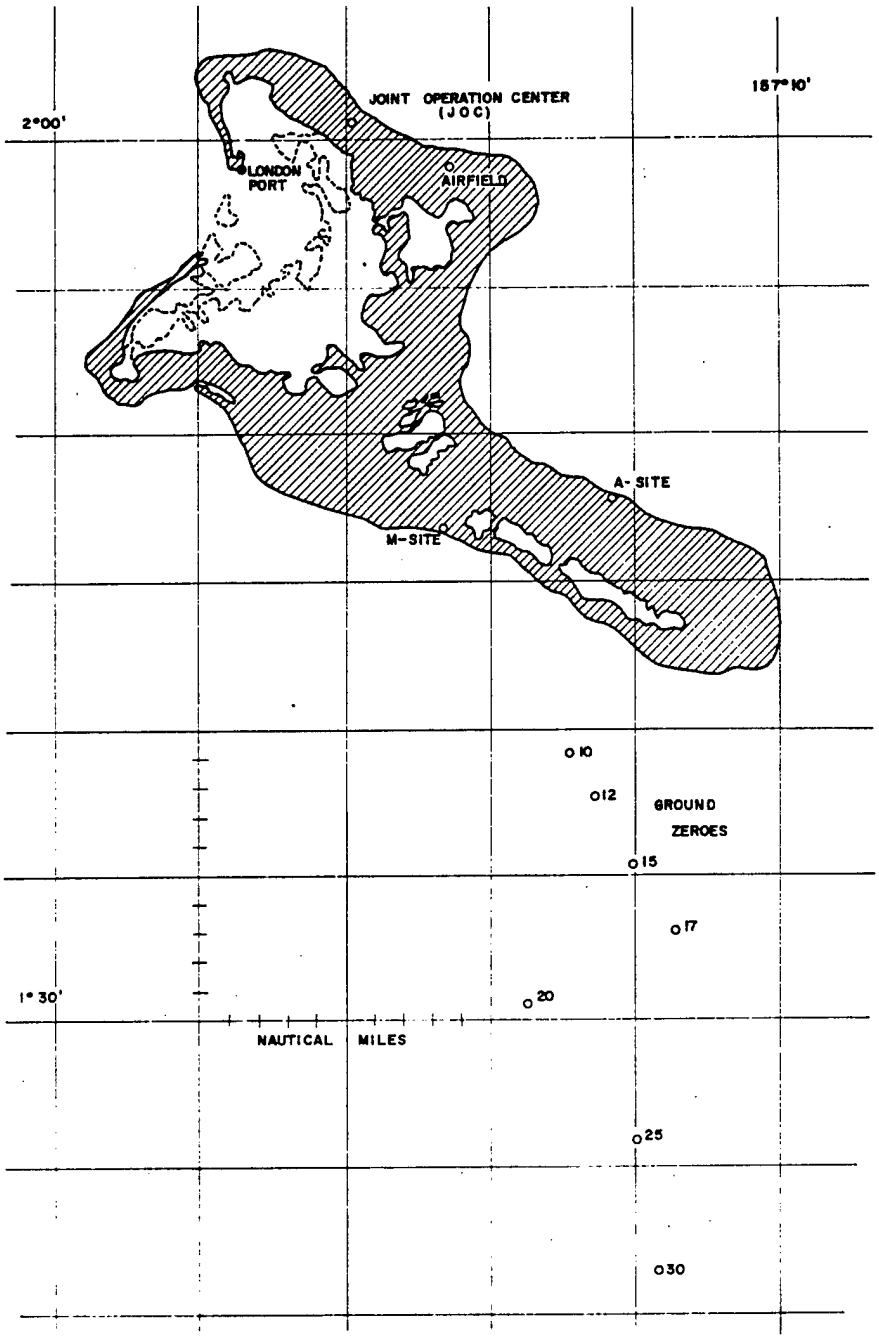

Fig. 1 Map of Christmas Island.

Pressure recordings were made on Visicorder oscilloscopes at 1-inch/second paper speeds and with about 1-inch deflections for gage-rated pressures. Some typical pressure traces are shown in Fig. 2.

At the beginning of the operation, gage bleed plugs were erroneously left open for the first two shots. Recordings showed only approximate amplitudes for the first sharp pressure rise. This was corrected, but some leakage past gage O-rings persisted for the next few shots. By Shot 6 (Yukon), repairs were made and correct pressure times were being recorded.

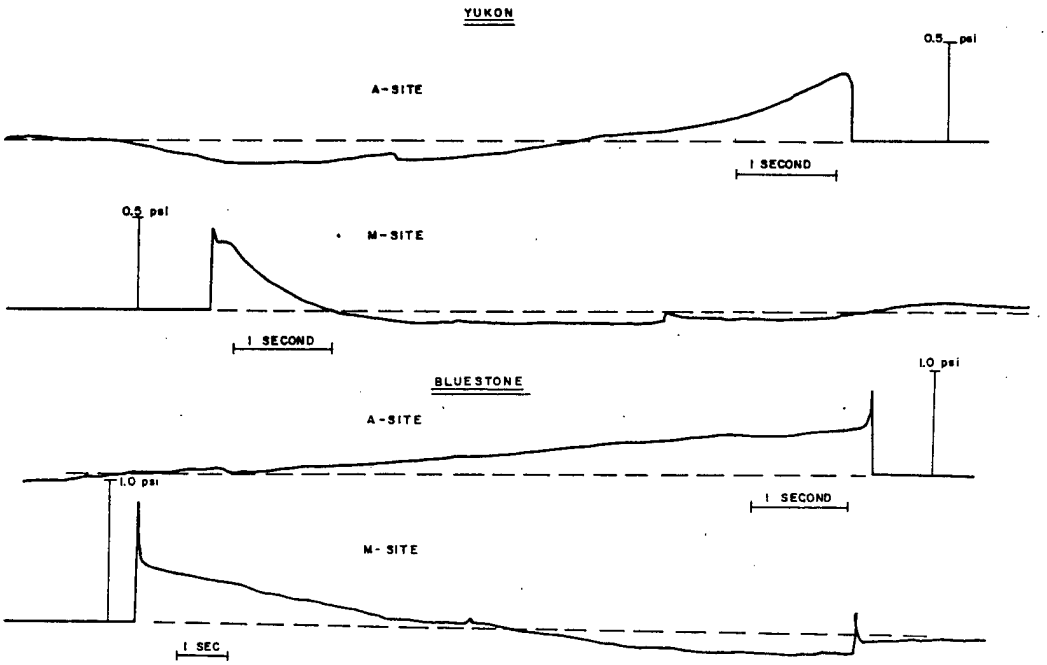

Fig. 2 Typical Wiancko gage pressure-time records.

Sharp pressure spikes were recorded at shock arrival on many occasions. At first these were believed to be gage or recorder ringing, but this was discounted when occurrences were intermittent and did not correlate with station or overpressure. Finally, on the last three shots, signals at A site were recorded on photos of an oscilloscope tube to resolve the spike duration. These are reproduced in Fig. 3 and show clearly that spike durations are several milliseconds. Instrument oscillations were also noted, but they are restricted to the first fraction of a millisecond. It is concluded that spikes shown on slow-speed records are real pressure phenomena, with space dimensions (several feet) larger than could have been caused by any reflective material near the sensors.

Microbarographs operated at JOC and London were similar to those used for years in recording nuclear tests.[5,6] Differential-pressure wave sensors were twisted Bourdon tubes which turned an armature with respect to an E-core, varying reluctance to modulate a carrier wave transmitted by coaxial line into appropriate signal amplifiers for recordings. Sensors were produced by Wiancko Corporation, Pasadena, California, as specified and evaluated by Sandia Laboratory.[7] Amplifier systems in current use were designed at Sandia and built by the Electronic Engineering Company, Santa Ana, California. Brush Electronics Company pen-type recorders were used at a paper speed of 2.5 centimeters per second. One-second time marks were made by an event-marking pen. Zero-time and count-down time signals were recorded on each pressure trace as received from the public address system. Combined instrument and recorder response time for pressure signals was such that 95 percent of pen deflection from a square-wave pressure pulse would be recorded in about 15 milliseconds. Thus, there is minimum amplitude damping for signals with frequencies lower than 10 cps.

A Site

Oscilloscope Time Scale

BLUESTONE	SUNSET
0.5 millisecond/centimeter	2 milliseconds/centimeter
4.5 msec recorded	13 msec recorded

Fig. 3 Scope photos of shock wave arrival gage pressures.

Sandia microbarographs have seven set-range switch positions which allow signal amplitudes from 1 microbar to 48 millibars to be satisfactorily recorded, provided that wind noise at low signal levels and blast damage at high pressure levels are not excessive. Recent calibration tests have shown that about 85 percent of previous recordings were accurate to ±20 percent. Typical microbarograph recordings are shown in Fig. 4.

Pressure sensors for microbarographs were not ideally exposed, but nearby buildings and trees should not have significantly affected results from these relatively slow-compressing, long-duration waves at tens of miles range.

Most previous air burst experience was gained in Nevada with morning shots, where strong temperature inversions caused different shock or sound propagation patterns. Measurements from previous operations also gave no clear indication that spiking phenomena would be observed. Measurements of Ivy King shot were subject to instrumentation difficulties: some gages were overdamped, some gages were underdamped, and these difficulties in high-pressure, fast-rise signal regions obscured significant spike recording. This was reported by Rolloson in WT-602.[3] Also, in a Hardtack report, WT-1612,[2] Ballistics Research Laboratories (BRL) information showed many measurements at low pressures, but these were from surface-burst tests. Self-recording, very low-pressure gages were used by BRL, and sufficiently accurate pressure-record reproductions showing significant spike information were not secured. Furthermore, a review of high-explosive experiments with HOB effects at Sandia Laboratory conducted during the period from 1953 to 1956 did not show positive indication of spikes.[8,9] A spike shown on these Sandia 256-pound HE records, provided the spike was a scalable time quantity, would have had much too short a duration to have been recorded.

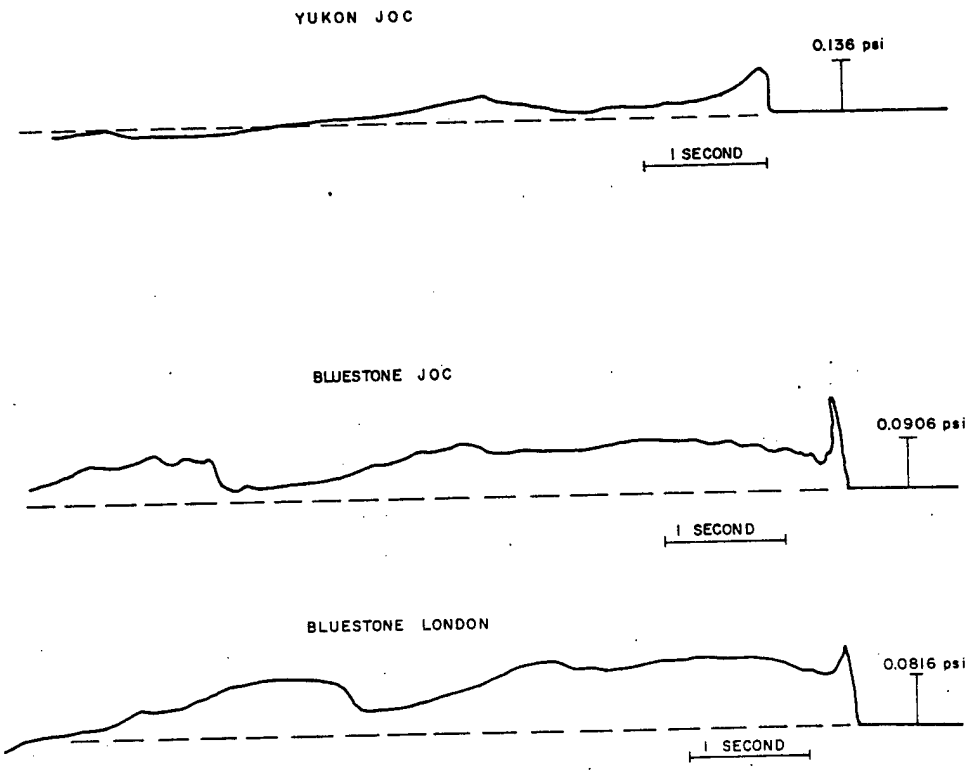

Fig. 4 Typical microbarograph pressure records.

On the other hand, some very small scale measurements of hill-and-dale effects by Todd and Schellenbaum[10] showed that on the fore-face of a hill, spiking would occur. From this approach spiking may result, not from hill-and-dale effects at Christmas Island, of course, but from atmospheric refractive bending which could conceivably generate a virtual hill-and-dale effect.

In SC-4037,[11] Martha Stickel showed that among height-of-burst effects there may be an extension of positive-phase duration coinciding with the reduction in positive-phase impulse, explained by a concavity upward of the pressure-time trace which could eventually result in a sharp spike. She also shows some correlation of this anomalous pressure decay with occurrence of the "Pete" wave, either in or near the negative pressure phase.

Lincoln Smith's studies at Princeton, reported in NDRC-A-350,[12] (shock tube studies on reflection of plane shocks in air) indicated that at some critical wave incidence angles to a large reflecting plate there would be very high pressure concentrated in some areas associated with triple point formation. Also, there was indication of strong rarification waves behind the triple point formation which might result in pressure-spike generation. However, Smith's pressure-time gages could not be constructed small enough nor provide adequate response characteristics to positively record this anomalously high pressure which theory led him to expect at critical incidence angles. In full-scale testing there has been no observation of this effect. This may have been because full-scale tests were conducted over real ground terrain where small-scale irregularities may have attenuated high frequencies which contribute to spike formation.

Another study of height-of-burst effects at long ranges was made at Sandia Laboratory by Church.[13] His report showed that height-of-burst effects were propagated by the ozonosphere at least to the ground level sound ring near a distance of 150 miles. Experiences at Christmas Island did not appear to show that height-of-burst effects of enhanced overpressures were propagated even to 40 miles distance, but it was believed that this apparent shortcoming was strongly influenced by atmospheric effects.

Preliminary field studies of sound-ray paths from Christmas Island tests showed only weak correlation between scaled signal amplitude and height of a refracted wave passing over the instrumentation. Meteorological measurements were probably not adequately accurate or representative for true sound-ray calculation and strong correlation with observed pressures. Thus the task of evaluating Christmas Island data is difficult. The following approaches were used: (1) meteorological balloon observations were employed, (2) sound-ray paths were calculated, and (3) apparent pressure reductions or enhancements at Sandia observation stations were correlated with ground strike range of the calculated refracted limiting ray. True pressure-distance decay curves in the computed ray region and diffracted decay curves in the so-called "silent" regions were (hopefully) separated.

Preliminary values of burst location, burst height, and fireball yield were used in many of the calculations. Subsequent refinements of such of these values as are now available will only slightly affect results of this study.

3 RESULTS

3.1 Measurements

Shot data for the 24 aircraft drops at Christmas Island are shown in Table 1. Yields, heights of burst, and ground coordinates were obtained from LAMS-2757.[14] Values for cube root of yield and 1-kt scaled height of burst are also listed. Apparent yield is the free-air-burst yield required to give the same overpressure as was given by the actual yield and burst height. The ratio of apparent to actual yield versus scaled burst height is graphed is Fig. 5. Two curves, one interpreted from data in TM 23-200[1] and one from SC-3858,[8] are shown as derived from conditions at 2000 feet range from a 1-kiloton burst.

Height-of-burst pressure enhancement effects are well conserved in further propagation out to at least 150 miles. This was demonstrated by microbarograph pressure comparisons between high-explosive bursts at 0, 0.2, 1, and 3 ft/(lb HE)$^{1/3}$ in a series of experiments at Sandia Laboratory in 1961.[13] Therefore, height-of-burst effects for Sandia Dominic data at intermediate ranges of 10 to 40 miles should be the same.

The final data column in Table 1 shows the proportionality constant in the predicted standard overpressure-distance equation, $\Delta p = kR^{-1.2}$, for Δp in psi and R in kilofeet. Range to a given overpressure is scaled to vary with the cube root of apparent yield, and for a given yield overpressure is inversely proportional to the 1.2-power of the range for $\Delta p \leq 0.37$ psi. For $\Delta p > 0.37$ psi the overpressure-distance curve from IBM Problem M calculations[15] is used for standard scaled predictions. The -1.2 exponent on range for low pressures was found valid in May 1961 for 1-pound pentolite spheres to 500 feet range in experiments at Sandia's Coyote Canyon Test Field. It was further verified to 80,000 feet from 500-pound pentolite spheres in Project Banshee at White Sands Missile Range during July and August, 1961.[16] In each of these experiments, measurements were made at ground zero beneath

TABLE 1 SHOT DATA SUMMARY

Shot	Date	Yield (kt)	$W^{1/3}$	Coordinates N (m)	Coordinates E (m)	HOB(ft)	1-kt scaled HOB(ft)	Apparent yield W_A(kt)	Standard $R^{1.2}\Delta p$	Remarks
1 - Adobe	4/25	190	5.75	180,790	691,810	2730	475	529	63.4	
2 - Aztec	4/27	408	7.41	181,067	691.522	2610	352	909	79.3	
3 - Arkansas	5/2	1090	10.29	175,340	693,550	5030	488	3080	129.0	
4 - Questa	5/4	670	8.75	174,117	695,728	5230	598	2350	115.6	
6 - Yukon	5/8	119	4.92	181,245	691,910	2880	586	467	60.4	
7 - Mesilla	5/9	69	4.10	181,565	691,850	2450	598	242	46.6	
8 - Muskegon	5/11	50.4	3.69	182,040	690,700	2995	810	256	47.5	
10 - Encino	5/12	512	8.00	179,990	690,870	5510	690	2150	111.3	
11 - Swanee	5/14	97	4.59	182,320	690,640	2940	640	369	54.9	
12 - Chetco	5/19	77.6	4.26	182,495	690,180	6905	1620	159.8*	39.4	TM-23-200
13 - Tanana	5/25	2.3	1.32	182,590	690,410	9030	6840	2.3	14.45	free air burst
14 - Nambe	5/27	42.5	3.49	182,570	690,335	7140	2042	42.5	46.4	free air burst
15 - Alma	6/8	807	9.31	176,570	693,675	8865	952	4520	150.1	
16 - Truckee	6/9	225	6.08	182,305	690,935	6970	1147	923 *	79.7	TM-23-200
17 - Yeso	6/10	3130	14.65	166,750	686,695	8235	562	10230	208.5	
18 - Harlem	6/12	1100	10.32	171,535	694,910	13645	1323	3530 *	135.8	TM-23-200
19 - Rinconada	6/15	815	9.33	171,825	695,120	9105	977	4560	150.2	
20 - Dulce	6/17	54.3	3.79	182,800	689,165	9090	2396	54.3	51.3	free air burst
21 - Petit	6/19	2.1	1.28	172,165	695,925	14995	11710	2.1	13.93	free air burst
22 - Otowi	6/22	81.5	4.34	182,060	689,750	9010	2076	81.5	60.3	free air burst
23 - Bighorn	6/27	7650	19.71	151,415	693,360	11810	599	26850	335.0	
24 - Bluestone	6/30	1270	10.83	171,470	695,058	4980	460	3430	134.7	
26 - Sunset	7/10	810	9.32	171,600	695,185	5000	536	2520	118.2	
27 - Pamlico	7/11	3820	15.63	157,780	694,510	14330	916	21000	278.5	

*Note: TM-23-200 HOB data used for $10 < \lambda < 20$; free-air-burst reflected pressure predicted for $\lambda > 20$.

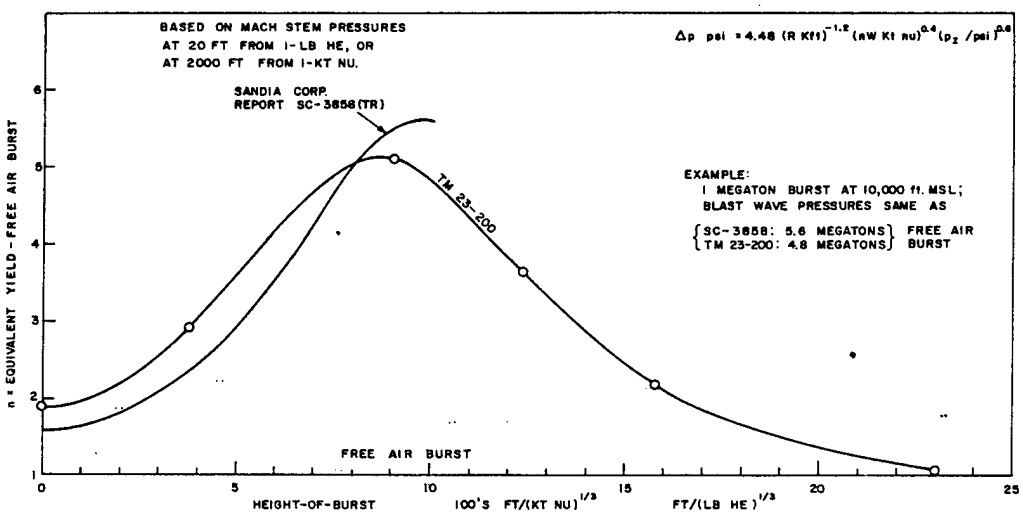

Fig. 5 Height-of-burst effects on equivalent blast yield for overpressure predictions.

high bursts to remove any possible attenuation or interference effects from atmospheric refraction. The reference standard overpressure-distance curve for a 1-kt nuclear free air burst at sea level is shown in Fig. 6.

Table 2 summarizes the primary measurements made from Sandia pressure recordings. For each shot and recording station are entries for shot range, sharp rise pressure change, solid overpressure (defined as peak overpressure after spikes have been removed), maximum negative-phase pressure, positive pressure pulse duration, and negative-phase duration. Predicted standard peak overpressures are shown for comparison with observations. Scaled ranges and positive-phase durations are also shown for 1-kt free air bursts. Sketches of observed pressure-time traces are included in the remarks column.

3.2 Directional Dependence

Site A and Site M were at nearly equal ranges from each of the shot targets, as were JOC and London. All stations were in the north quadrant from shots and approximately crosswind of the prevailing tradewind circulation. The small wind components directed toward or away from the gage stations were not expected to cause significant blast propagation variations. There were, however, numerous occasional differences between measurements made at Site A and Site M which were separated by 39 degrees in bearing, and even between JOC and London which were separated by only 10 degrees in bearing.

Comparisons of overpressures between Site A and Site M are displayed in Fig. 7. Both sharp rise pressures (open circles) and solid overpressures (solid circles) are compared and connected. There does not appear to be any regular and consistent relationship between the ratio of solid pressure observations and the ratio of sharp rise pressure observations. There is, however, less difference between A and M solid pressures than between their sharp rise or spike values. This is shown by both the average relationships and the standard deviations. Assuming a logarithmic normal distribution for the data, as is often appropriate for data having large proportional deviations and several orders of

TABLE 2 BLAST PRESSURE DATA SUMMARY

Shot	Station	Range (kft)	Fast pressure increase (psi)		Solid over-pressure (psi)	Peak negative pressure (psi)	Positive-phase duration (sec)
1 - Adobe	A	58.5	0.270*		-	-	-
	M	60.3	0.514*		-	-	-
	J	145.2	0.1243	=	0.1243	0.0297	4.01
2 - Aztec	A	57.9	0.266*		-	-	-
	M	59.5	0.640	=	0.640	-	-
	J	144.0	0.0979		0.1595	0.0635	4.13
3 - Arkansas	A	76.5	0.536		0.552	0.192	6.31
	M	79.0	0.507		0.456	0.109*	-
	J	165.9	0.0419		0.0896	0.0720	8.97
4 - Questa	A	81.0	0.526	=	0.526	0.140	4.64
	M	86.0	0.535	=	0.535	0.093*	4.61*
	J	170.3	0.0895		0.1187	0.0409	4.74
6 - Yukon	A	56.9	0.304		0.338	0.110	3.23
	M	59.5	0.428	=	0.428	0.110*	2.71*
	J	143.9	0.1250	=	0.1250	0.0286	3.44
7 - Mesilla	A	59.6	0.152		0.192	0.072	2.32
	M	58.5	0.430		0.286	0.078	2.20*
	J	142.9	0.0326		0.0431	0.0198	3.29
8 - Muskegon	A	55.0	0.270		0.156	0.082	2.23
	M	55.4	0.400		0.217	0.090	2.00
	J	140.1	0.0226		0.0675	0.0216	2.09
10 - Encino	A	61.5	0.614		0.498	0.180	4.20
	M	61.5	0.940		0.763	0.204	3.96
	L	146.7	0.1678		0.1412	0.0720	4.50
	J	146.6	0.1322		0.1248	0.0648	4.44
11 - Swanee	A	53.8	0.377		0.200	0.070	2.81
	M	54.3	0.342		0.249	0.082	2.53
	L	139.7	0.0461		0.0304	0.0245	5.46
	J	139.2	0.0259		0.0429	0.0196	5.66
12 - Chetco	M	53.6	0.500		0.336	0.130	2.17
	L	138.5	0.0650		0.0530	0.0407	2.83
	J	138.1	0.0344		0.0462	0.0331	3.57
13 - Tanana	A	53.6	0.099	=	0.099	0.108	0.45
	M	53.8	0.144	=	0.144	0.046	0.79
	L	138.6	0.0136	=	0.0136	0.0109	0.92
	J	138.1	0.00924	=	0.00924	0.00780	1.23
14 - Nambe	A	53.0	0.327		0.287	0.071	2.17
	M	53.5	0.674		0.346	0.082	1.67
	L	138.5	0.0782		0.0681	0.0143	1.55
	J	138.0	0.0611		0.0550	0.0144	2.21

*Bleed plug open or not well sealed.

TABLE 2 BLAST PRESSURE DATA SUMMARY (Cont)

Negative-phase duration (sec)	Scaled range (kft)	Standard over-pressure (psi)	Predicted diffracted overpressure (psi)	Remarks
-	10.2	0.480		*
-	10.5	0.462		*
12.48	25.2	0.160	0.074	
-	7.8	0.606	0.29	*
-	8.0	0.586		*
8.63	19.4	0.202	0.069	
10.20	7.4	0.704	0.41	
-	7.7	0.678		*
12.64	15.9	0.284	0.143	
9.14	9.3	0.590	0.37	
9.06*	9.8	0.549	0.47	*
10.96	19.5	0.243	0.118	
4.84	11.5	0.474	0.275	
5.15*	12.1	0.446		*
6.96	29.2	0.154	0.110	
7.12	14.5	0.345	0.150	
4.54*	14.3	0.350		*
8.11	34.8	0.120	0.055	
4.26	14.9	0.385	0.217	
6.05	15.0	0.382		
4.79	38.0	0.125	0.059	
8.60	7.7	0.791	0.75	
8.14	7.7	0.791		
9.46	18.3	0.281	0.150	
9.63	18.3	0.281	0.120	
5.55	11.7	0.458	0.24	
5.73	11.8	0.452	0.38	
Not repr.	30.4	0.145	0.060	
Not repr.	30.3	0.145	0.042	
4.67	12.6	0.329	0.32	A gage failed.
4.93	32.5	0.105	0.049	
5.94	32.4	0.105	0.043	
1.57	40.6	0.121	0.116	
1.31	40.8	0.121		
1.18	105.0	0.039	0.0203	
1.55	104.7	0.039	0.0178	
3.79	15.2	0.394	0.36	
3.69	15.3	0.390		
4.77	39.7	0.120	0.074	
6.09	39.5	0.120	0.090	

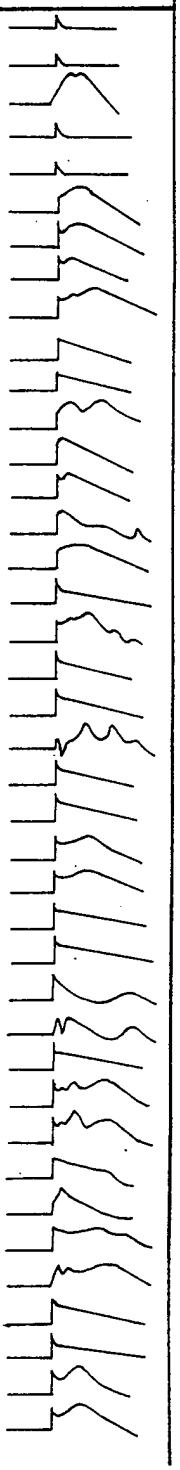

TABLE 2 BLAST PRESSURE DATA SUMMARY (Cont)

Shot	Station	Range (kft)	Fast pressure increase (psi)		Solid over-pressure (psi)	Peak negative pressure (psi)	Positive-phase duration (sec)
15 - Alma	A	71.9	1.061		0.614	-	-
	M	76.8	0.577		0.534	0.154	4.89
	L	161.0	0.1667		0.1197	0.0598	6.16
	J	160.3	0.2265		0.0840	0.0429	7.10
16 - Truckee	A	56.8	0.672		0.384	0.122	3.01
	M	55.3	0.587		0.483	0.149	2.86
	L	140.2	-		0.782	0.0437	4.40
	J	139.5	0.0277		0.0697	0.0376	4.20
17 - Yeso	A	106.8	0.222		0.436	0.120	8.70
	M	99.5	0.418		0.565	0.222	8.43
	L	181.3	0.1665		-	0.0966	-
	J	185.2	0.0257		0.1725	0.0706	9.44
18 - Harlem	A	91.3	0.689		0.434	0.150	6.36
	M	94.2	1.024		0.620	0.190	5.87
	L	175.9	0.0670		0.1287	0.0713	-
	J	177.2	0.0758		0.1058	0.0608	7.54
19 - Rinconada	A	87.6	0.781		0.490	0.107	5.42
	M	92.3	0.924		0.592	0.135	5.05
	L	176.9	0.1530	=	0.1530	0.0696	6.67
	J	176.6	0.1311		0.1366	0.0555	5.93
20 - Dulce	A	54.1	0.554		0.402	0.114	1.96
	M	51.4	-		0.479	0.107	1.79
	L	135.6	0.0290		0.0523	0.0385	-
	J	136.1	0.0279		0.0461	0.0261	2.54
21 - Petit	A	88.5	0.076		0.032	0.032	0.88
	M	94.2	0.0254	=	0.0254	0.0114	1.01
	L	177.2	0.00402	=	0.00402	0.00080	1.46
	J	176.5	0.00529	=	0.00529	0.00264	oscill.
22 - Otowi	A	55.8	0.313		0.485	0.135	2.08
	M	54.3	0.784		0.655	0.136	2.86
	L	139.0	-		0.1137	0.0457	2.54
	J	139.0	-		0.0962	0.0382	2.25
23 - Bighorn	A	155.6	0.466		0.407	0.154	13.63
	M	155.2	0.246		0.402	0.167	13.54
	L	236.0	0.0139		0.1610	0.0898	12.89
	J	239.0	0.0204		0.1372	0.0661	14.85
24 - Bluestone	A	89.3	0.744		0.452	0.186	7.60
	M	92.5	0.890		0.460	0.194	7.26
	L	177.9	0.1321		0.1150	0.0800	6.52
	J	177.6	0.1693		0.0996	0.0670	7.66

TABLE 2 BLAST PRESSURE DATA SUMMARY (Cont)

Negative-phase duration (sec)	Scaled range (kft)	Standard over-pressure (psi)	Predicted diffracted over-pressure	Remarks
-	7.7	0.887		Recorder stopped by shock.
12.52	8.2	0.819		
12.03	17.3	0.337	0.226	
14.67	17.2	0.338	0.240	
6.93	9.3	0.625		
9.16	9.1	0.645		
12.82	23.1	0.209	0.178	Slow rise.
13.08	22.9	0.211	0.142	
16.50	7.3	0.764	0.47	
16.22	6.8	0.831	0.48	
-	12.4	0.403	0.142	Recorder stopped, peaks only.
17.43	12.6	0.394	0.138	
14.12	8.8	0.597	0.47	
12.88	9.1	0.576	0.54	
-	17.0	0.273	0.146	Timer out.
18.20	17.2	0.270	0.132	
14.29	9.4	0.700		
14.57	9.9	0.654		
14.23	19.0	0.301		
15.23	18.9	0.301		
8.15	14.2	0.423		
6.03	13.5	0.451		One gage failed.
-	35.7	0.141		Timer out.
5.57	35.9	0.141		
1.31	69.1	0.064		Very small deflection.
0.98	73.6	0.059		
2.89	138.4	0.028	0.0237	
-	137.9	0.028	0.0240	
6.52	12.9	0.482		
4.25	12.5	0.497		
5.20	32.1	0.160	0.113	Slow rise.
4.74	32.1	0.160	0.113	Slow rise.
20.49	7.9	0.782	0.375	One gage.
20.08	7.9	0.782	0.42	
20.21	12.0	0.479	0.167	
25.00	12.1	0.472	0.170	
14.43	8.2	0.613	0.47	
14.95	8.5	0.586	0.50	
8.87	16.4	0.270	0.135	
13.53	16.4	0.270	0.159	

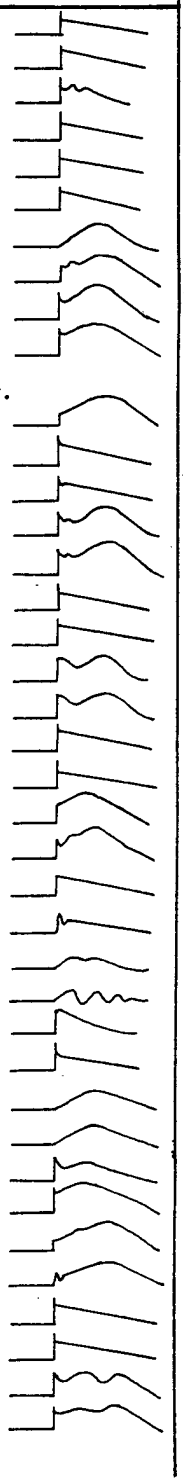

TABLE 2 BLAST PRESSURE DATA SUMMARY (Cont)

Shot	Station	Range (kft)	Fast pressure increase (psi)	Solid over-pressure (psi)	Peak negative pressure (psi)	Positive-phase duration (sec)
26 - Sunset	A	89.0	0.536	0.370	0.135	5.65
	M	92.6	0.724	0.342	0.114	5.85
	L	177.7	0.0480	0.0935	0.0809	6.36
	J	177.3	0.0509	0.0778	0.0713	5.93
27 - Pamlico	A	134.8	0.282	0.490	0.172	8.82
	M	134.4	0.443	0.442	0.144	8.96
	L	217.8	0.0908	0.2030	0.0939	8.25
	J	219.8	0.1014	0.1606	0.0799	9.62

TABLE 2 BLAST PRESSURE DATA SUMMARY (Cont)

Negative-phase duration (sec)	Scaled range (kft)	Standard over-pressure (psi)	Predicted diffracted over-pressure	Remarks
9.64	9.6	0.538	0.48	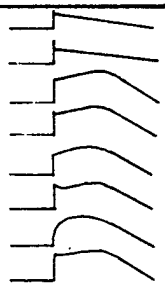
9.51	9.9	0.514		
11.37	19.1	0.236	0.155	
15.77	19.0	0.236	0.102	
17.74	8.6	0.759	0.51	
16.84	8.6	0.759	0.54	
14.02	13.9	0.435	0.205	
17.60	14.0	0.435	0.200	

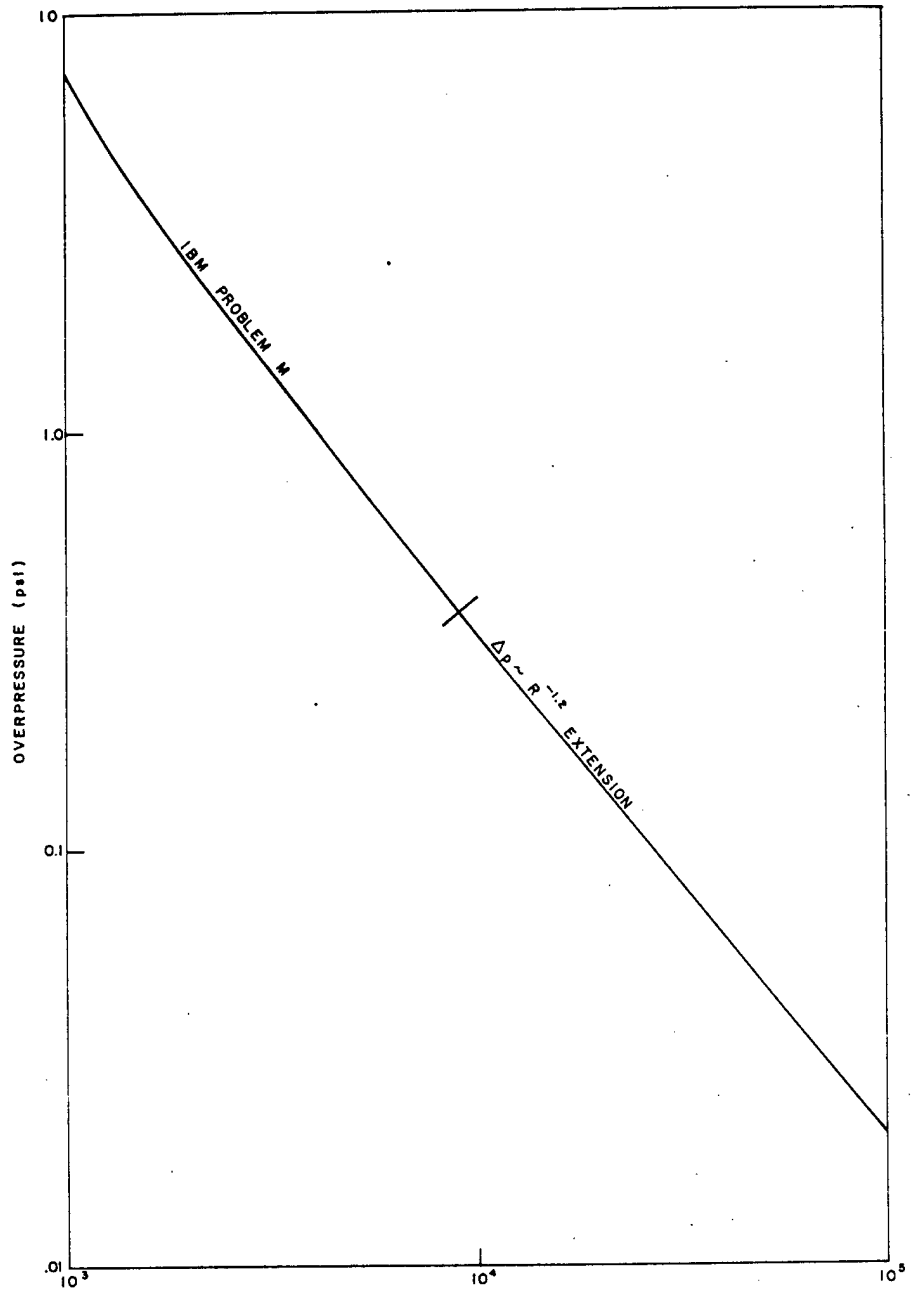

Fig. 6 Reference standard overpressure-distance curve.

magnitude range, the relationship may be expressed by

Sharp rise pressures: $A = 0.776M \times (2.02)^{\pm 1}$;

Solid overpressures: $A = 0.852M \times (1.21)^{\pm 1}$.

Pressure values at the respective instrument sites are designated as A and M. The expression $\times (2.02)^{\pm 1}$ indicates that plus-or-minus one standard deviation in the logarithmic normal distribution covers the range from $2.02 \times 0.776M = 1.566M$ to $0.766\ M/2.02 = 0.384M$. Sixty-eight percent of the A values will fall between $0.384M$ and $1.566M$. Such lack of correlation indicates that sharp rise

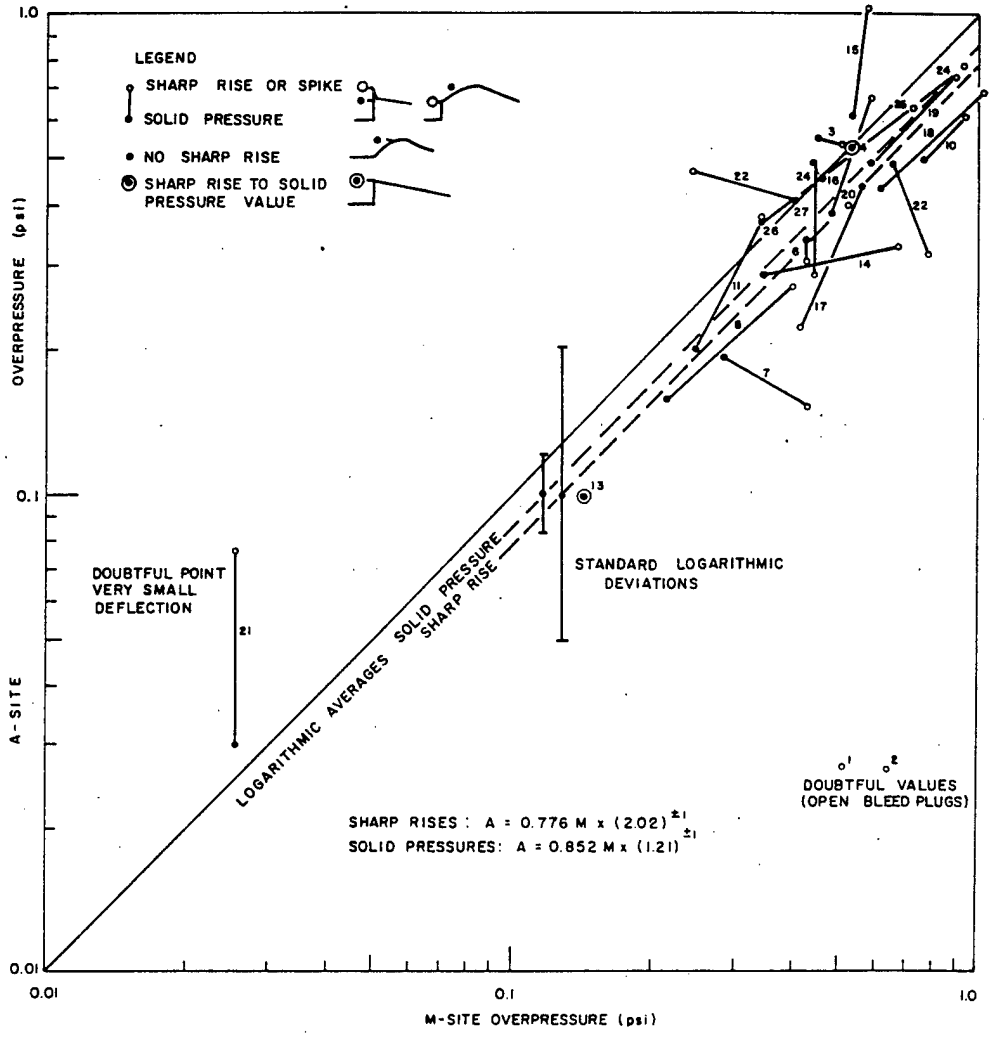

Fig. 7 Blast overpressure comparisons, A and M sites.

pressures may be quite dependent on local details of the propagating wind and air temperature field. Solid overpressures average 15 percent lower at A site than at M site, as might be expected, since A site is in a generally more upwind direction. There is less scatter in relating solid overpressures since effects of smaller scale atmospheric inhomogeneities are more nearly averaged over the long period of the blast wave. Differences between records at JOC and London are smaller, as shown in Fig. 8. This is probably caused by averaging effects of longer range propagation and the much smaller bearing angle difference.

It appears that verification and prediction refinements require separate approaches for sharp rise and solid pressures. Meteorological factors must be considered for each.

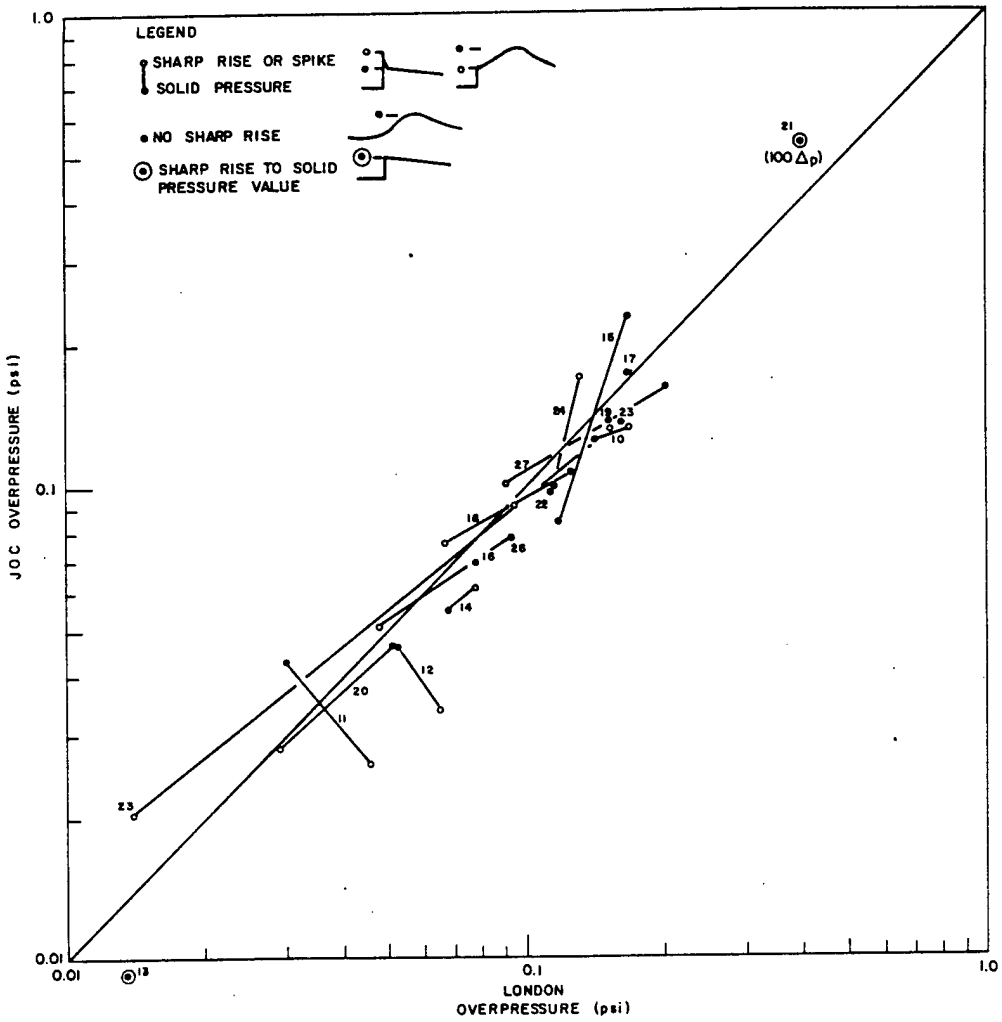

Fig. 8 Blast overpressure comparisons, London and Joint Operations Center.

3.3 Verification and Statistical Adjustment of Standard Predictions

Peak overpressures, Δp (spikes are neglected), have been plotted versus scaled range, $R/(W_A kt)^{1/3}$, for each of the four stations in Figs. 9, 10, 11, and 12. Several comparison curves are shown on each graph. Verification statistics (log normal) as related to these comparison standards are shown in Table 3.

TABLE 3 STATISTICAL COMPARISONS WITH STANDARDIZED PREDICTIONS

Station	Standard error factor	Mean ratio (observed standard)	Standard deviation around mean factor	Standard deviation around Christmas Island curve
A	1.598	0.674	1.288	1.360
M	1.424	0.824	1.344	1.535
JOC	2.601	0.424	1.524	1.602
London	2.243	0.461	1.262	1.369
Total				1.474

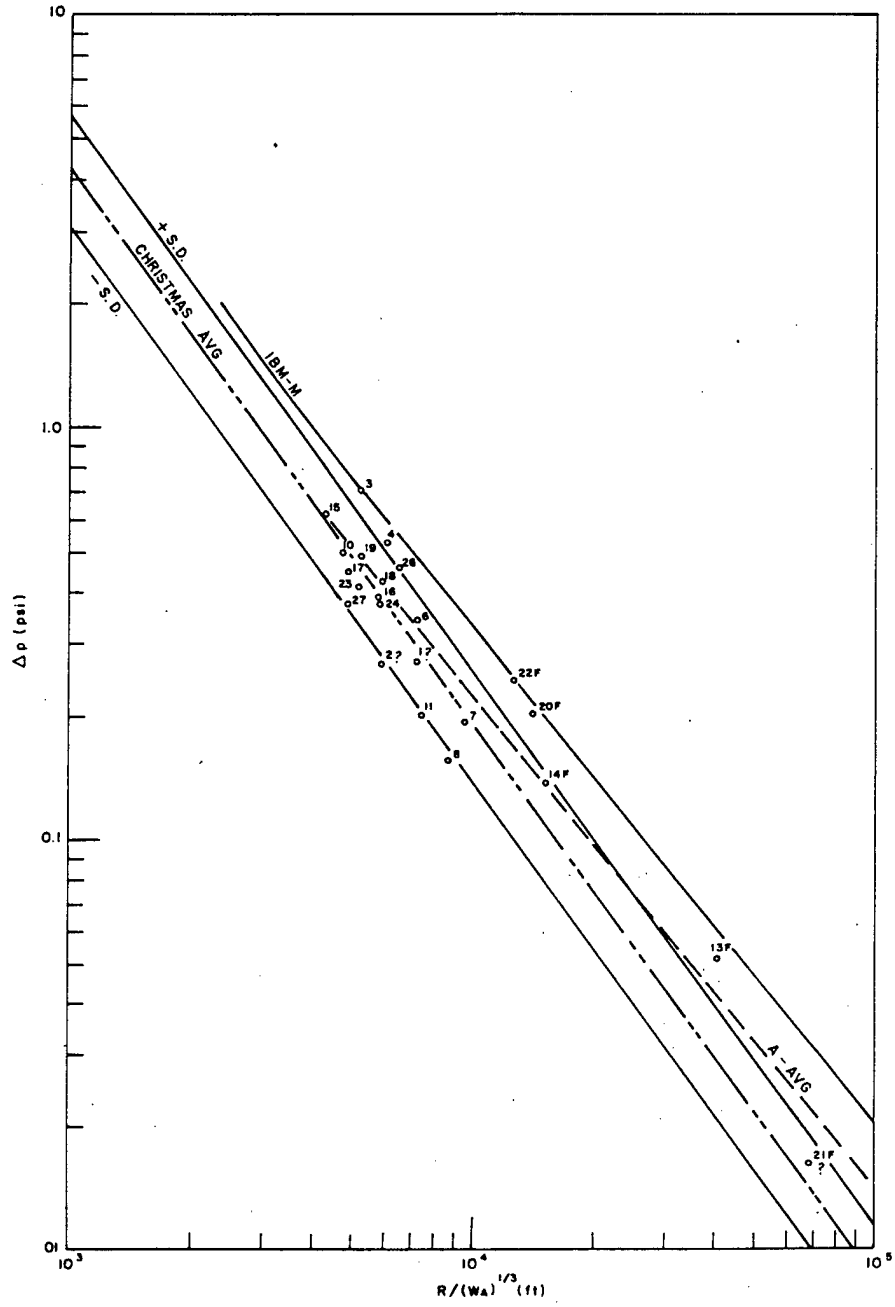

Fig. 9 Scaled overpressure-distance data, A site.

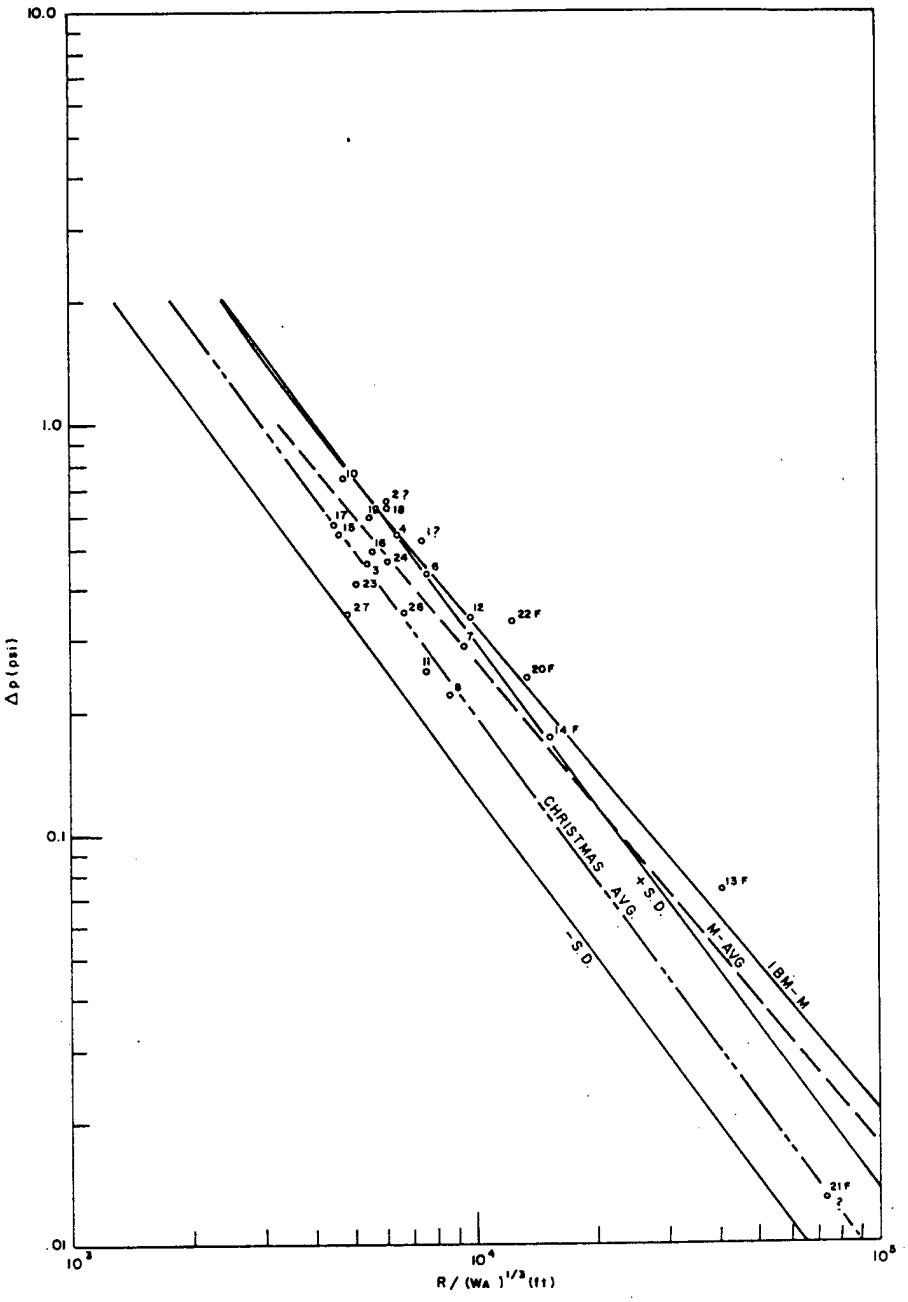

Fig. 10 Scaled overpressure-distance data, M site.

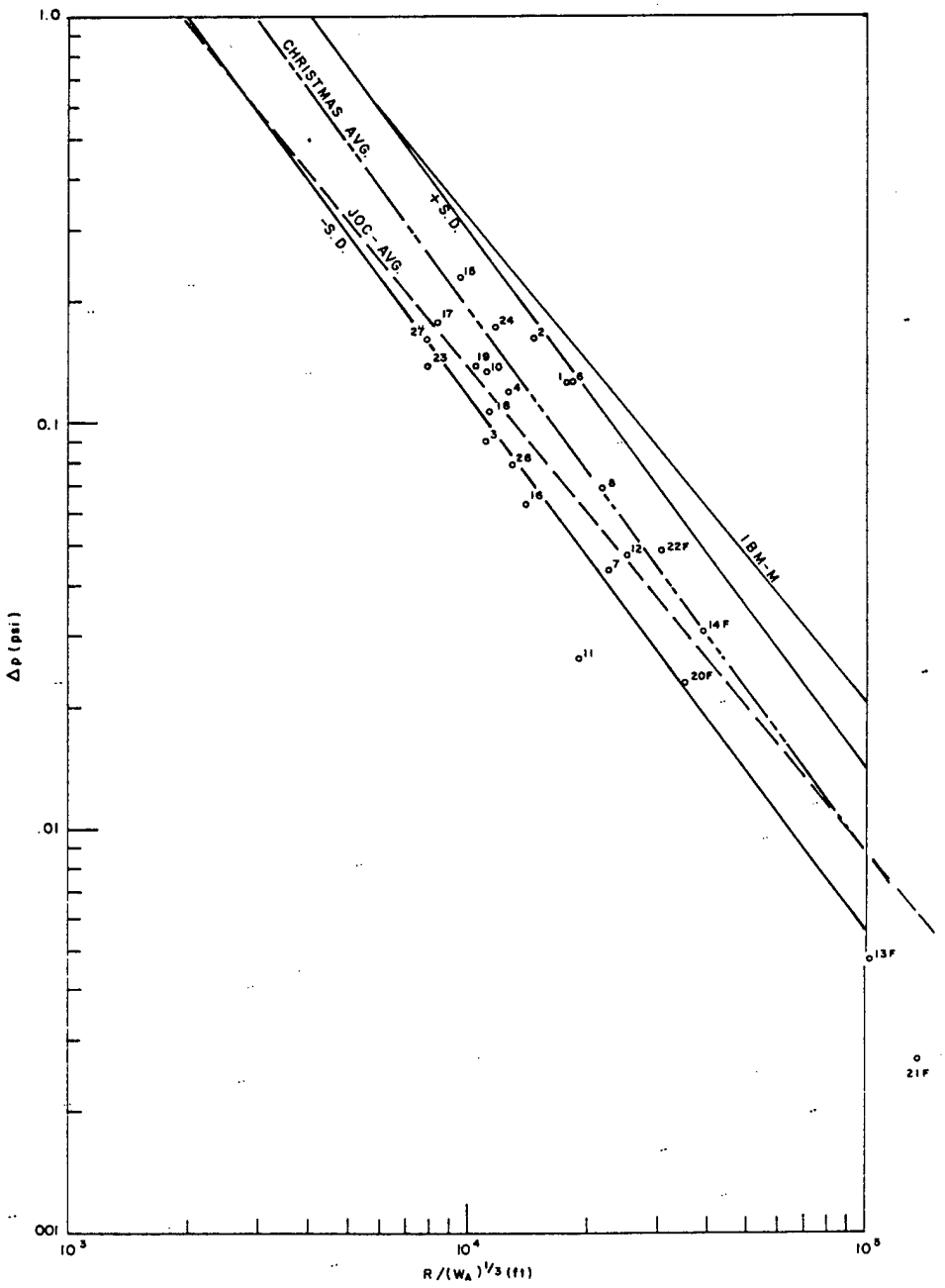

Fig. 11 Scaled overpressure-distance data, Joint Operation Center.

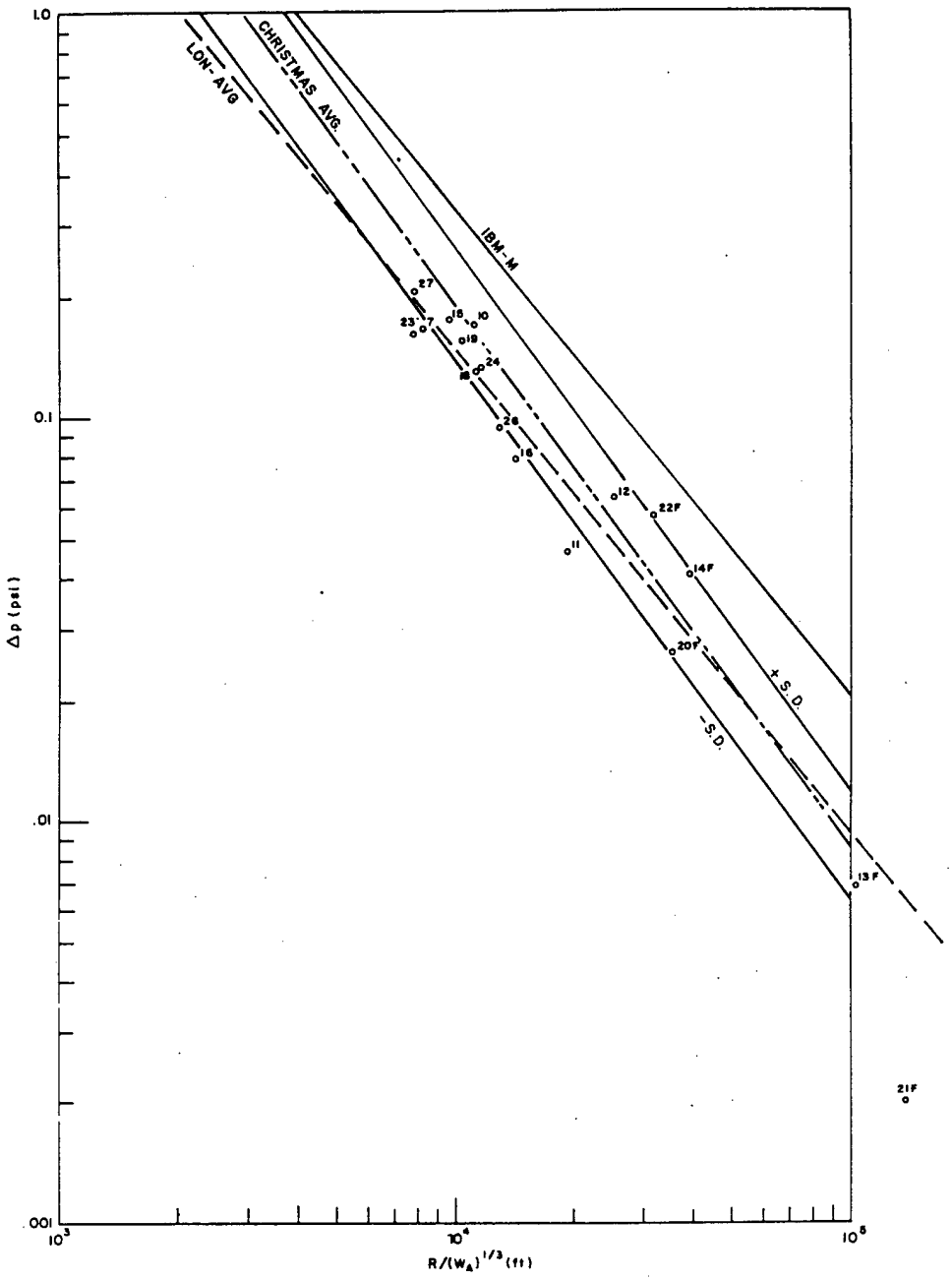

Fig. 12 Scaled overpressure-distance data, London.

The standard error factor, SE, is here defined for Δp_s = standard IBM-M overpressure and Δp_o = observed overpressure by

$$SE = \ell n^{-1}\left[\frac{1}{n}\sum_{i=1}^{i=n} \ell n^2\left(\frac{\Delta p_o}{\Delta p_s}\right)_i\right]^{1/2}.$$

The mean ratio between observed and standard overpressure is

$$\overline{(\Delta p_o/\Delta p_s)} = \ell n^{-1}\left[\frac{1}{n}\sum_{i=1}^{i=n} \ell n\left(\frac{\Delta p_o}{\Delta p_s}\right)_i\right].$$

Antilogarithm is understood to be represented by ℓn^{-1}. Standard deviation around the mean factor is

$$SD = \ell n^{-1}\left[\frac{1}{n}\sum_{i=1}^{i=n} \ell n^2\left(\frac{\Delta p_o}{\overline{(\Delta p_o/\Delta p_s)}}\right)\right].$$

The comparisons in Table 3 demonstrate that standard predictions would be significantly bettered by use of the mean factor for each station; means, however, were not available before the tests. A Christmas Island mean curve for overpressure versus distance for $10<R<40$ miles has been derived from the complete data set to show that

$$\Delta p = 4.24R^{-1.343},$$

which could be used without much more inaccuracy than is provided by station means. This equation, however, has not been derived for blast prediction use but for comparison with improved predictions which take into account meteorological conditions and may be applied elsewhere.

3.4 Atmospheric Refraction

Sound rays through the horizontally stratified atmosphere have been computed for each shot in the direction of each gage station. Ray calculations are as described in WT-9005.[6] These were performed on the CDC-1604 computer at Sandia Laboratory. It is assumed, with only small errors, that sound rays and shock rays follow the same paths through the atmosphere. Inputs to the calculation are burst height and a tabulation of heights, temperatures, and winds which were provided after each test by the JTF-8 Meteorological Center. Typical directed sound velocity-versus-height curves for the Alma and Bluestone events are shown in Fig. 13. Refracted sound-ray patterns for these shots are shown in Figs. 14 and 15.

On Shot Alma, direct rays hit A and M sites, but JOC and London were in the silent, or shadow, zone. Diffraction processes caused the observed blast pressures at these longer ranges. On the Bluestone event only diffracted signals reached any of the four stations. Similar calculations for all shots were made to obtain an overpressure-distance curve for diffracted waves.

At the maximum range of a direct ray, R_o, overpressure Δp_o was determined from the standard prediction curve scaled for yield and height of burst. Observed data points from shadow zones (Δp_1, R_1) were then used to plot $\ell n(R_o/R_1)$ versus $\ell n(\Delta p_o/\Delta p_1)$. An RMS line through these data showed that $\Delta p_o/\Delta p_1 = 0.789(R_o/R_1)^{-1.78}$. If a unit coefficient were assumed, i.e., standard overpressures would

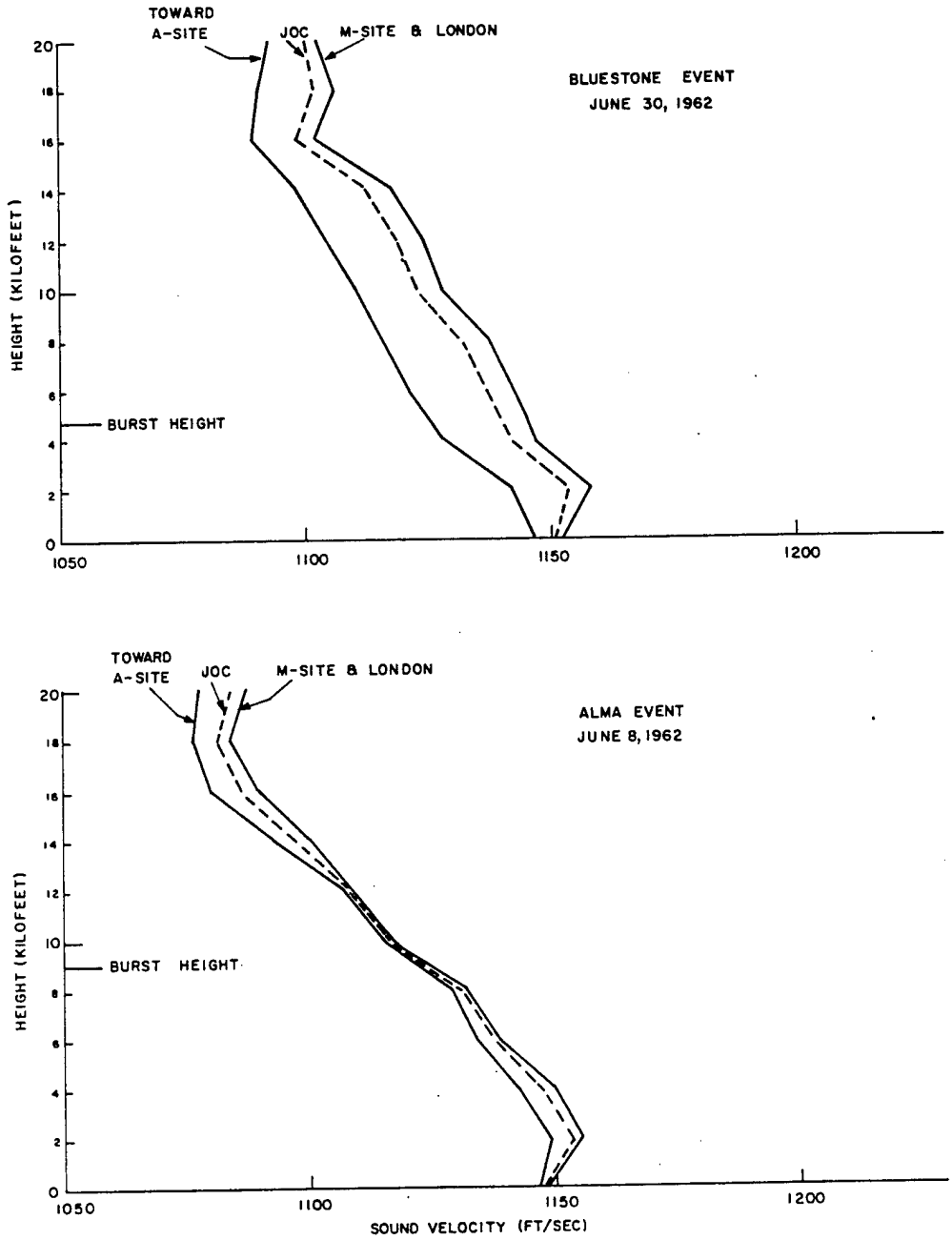

Fig. 13 Sound-velocity-versus-altitude curves, Bluestone and Alma events.

occur at ray strike ranges, and only the slope were allowed to vary, the RMS best-fit line gives $\Delta p_o/\Delta p_1 = (R_o/R_1)^{-2.03}$. For all practical purposes then, it may be concluded that overpressures in the shadow zone decay proportionally with the square of R_o/R_1.

This relationship for the shadow zone was applied to give the diffracted wave predictions column in Table 2. Pressure spikes at A and M sites were not included in deriving the diffracted wave curve but were used when they occurred at JOC or London. At the longer range stations equipped with slower

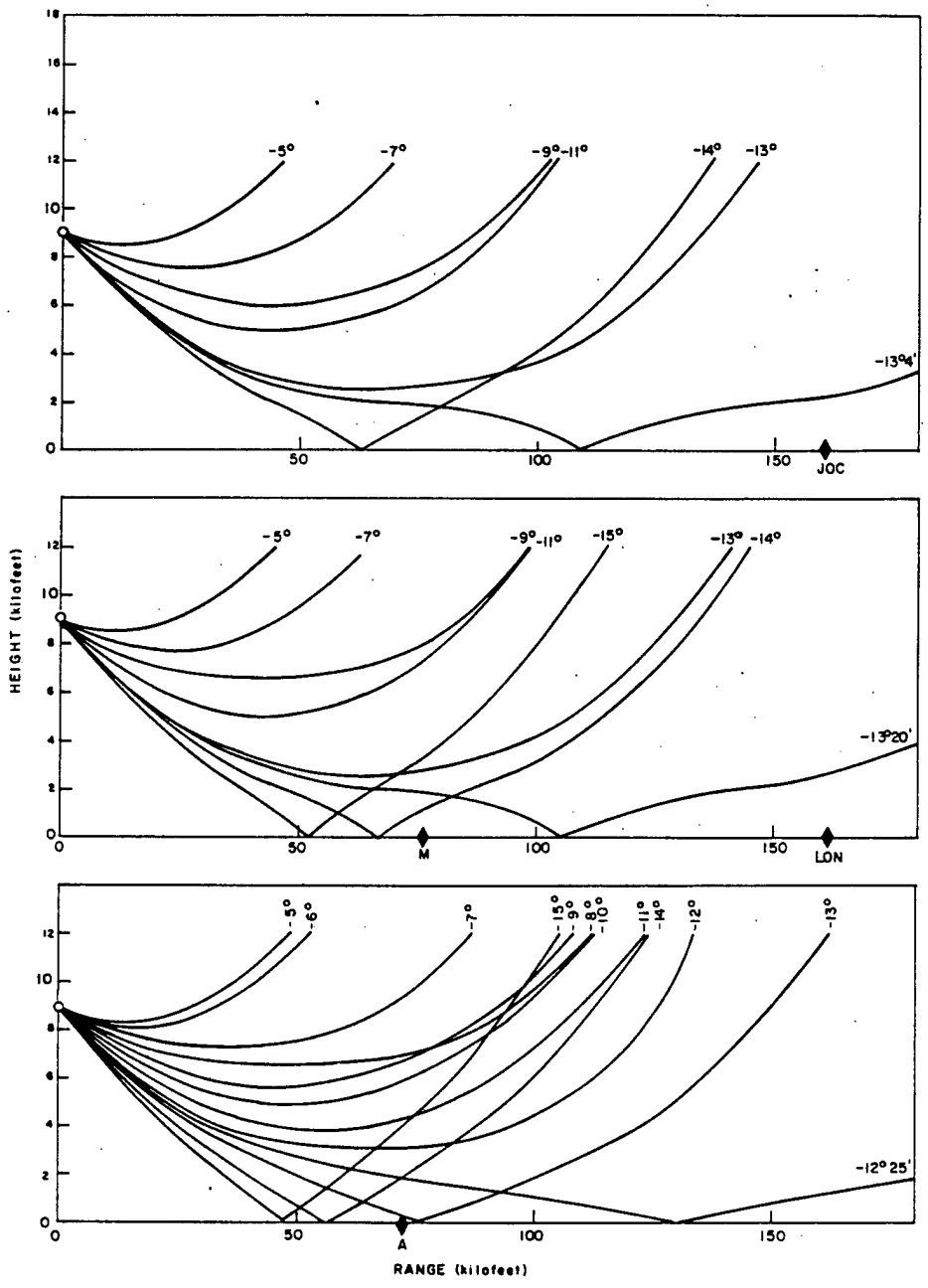

Fig. 14 Calculated refracted sound ray patterns, Alma event.

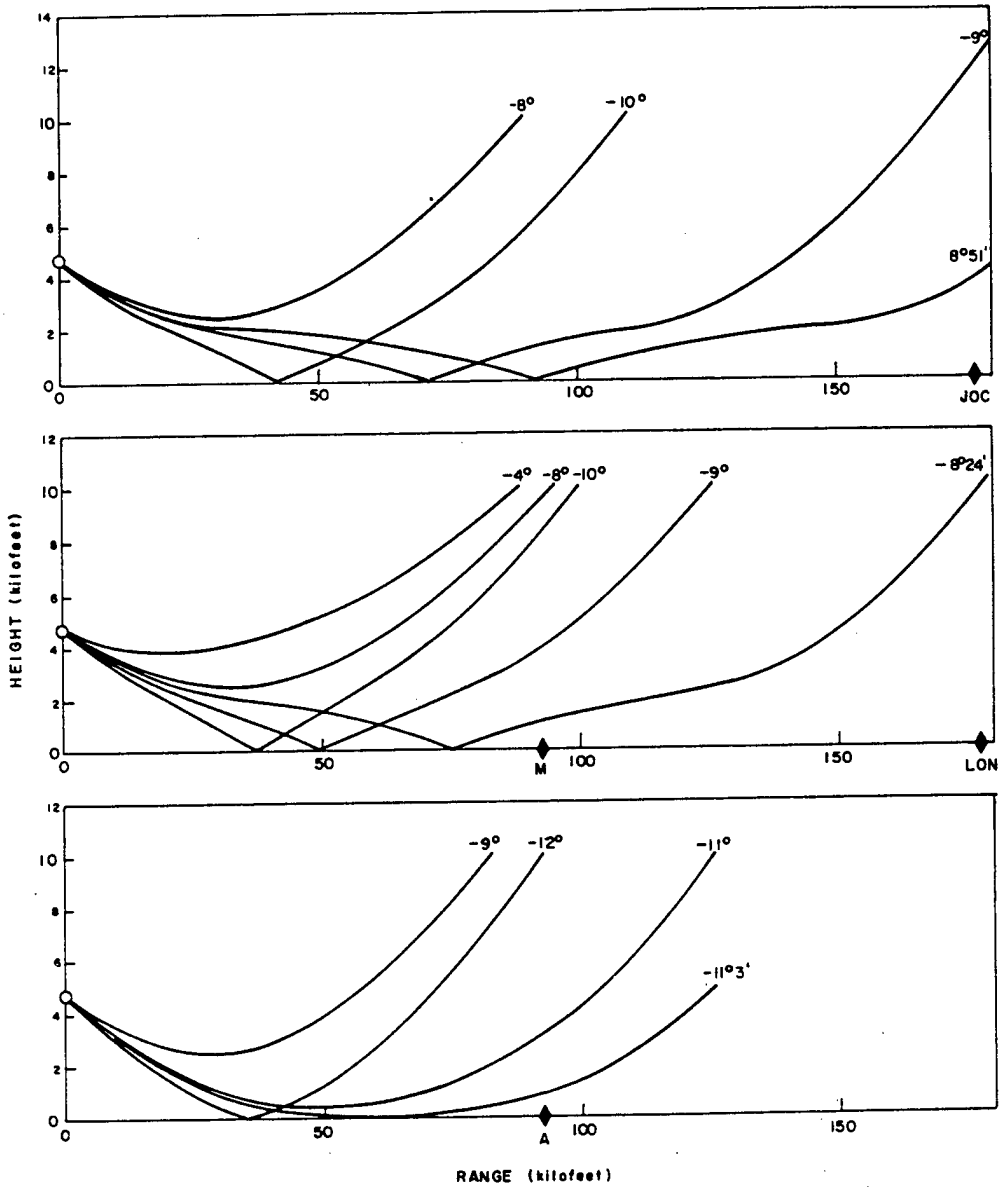

Fig. 15 Calculated refracted sound ray patterns, Bluestone event.

response sensors and recorders, observed spikes generally lasted nearly 0.1 second rather than the several milliseconds found at shorter ranges.

Pressure distance curve predictions for Alma and Bluestone are shown in Figs. 16 and 17, respectively. Lines are shown for standard free-air burst and for actual height of burst. Diffracted wave curves are dashed to show revised prediction based on meteorological influences at various station ranges. Observed data points are shown for both spike and solid overpressures.

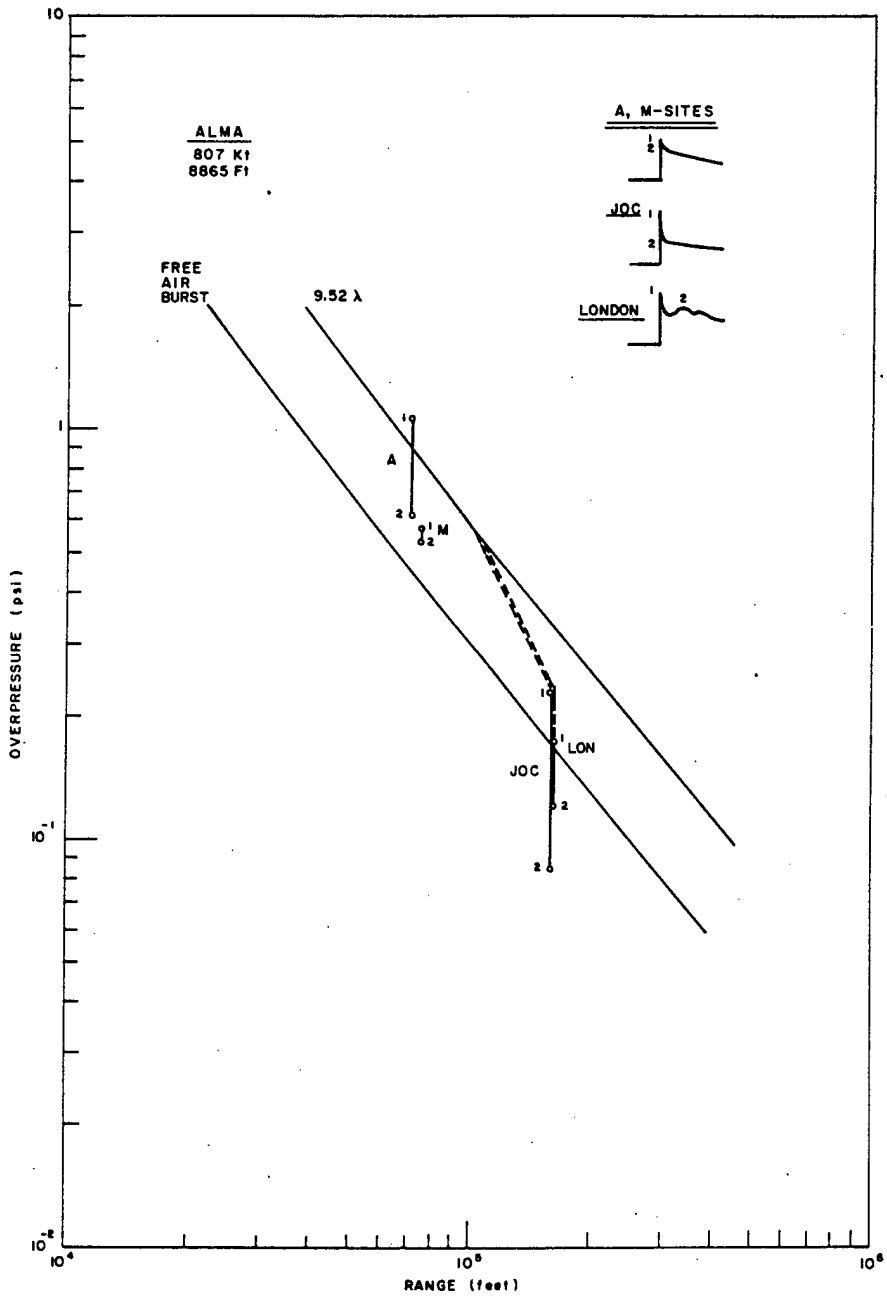

Fig. 16 Overpressure-distance calculations and measurements, Alma event.

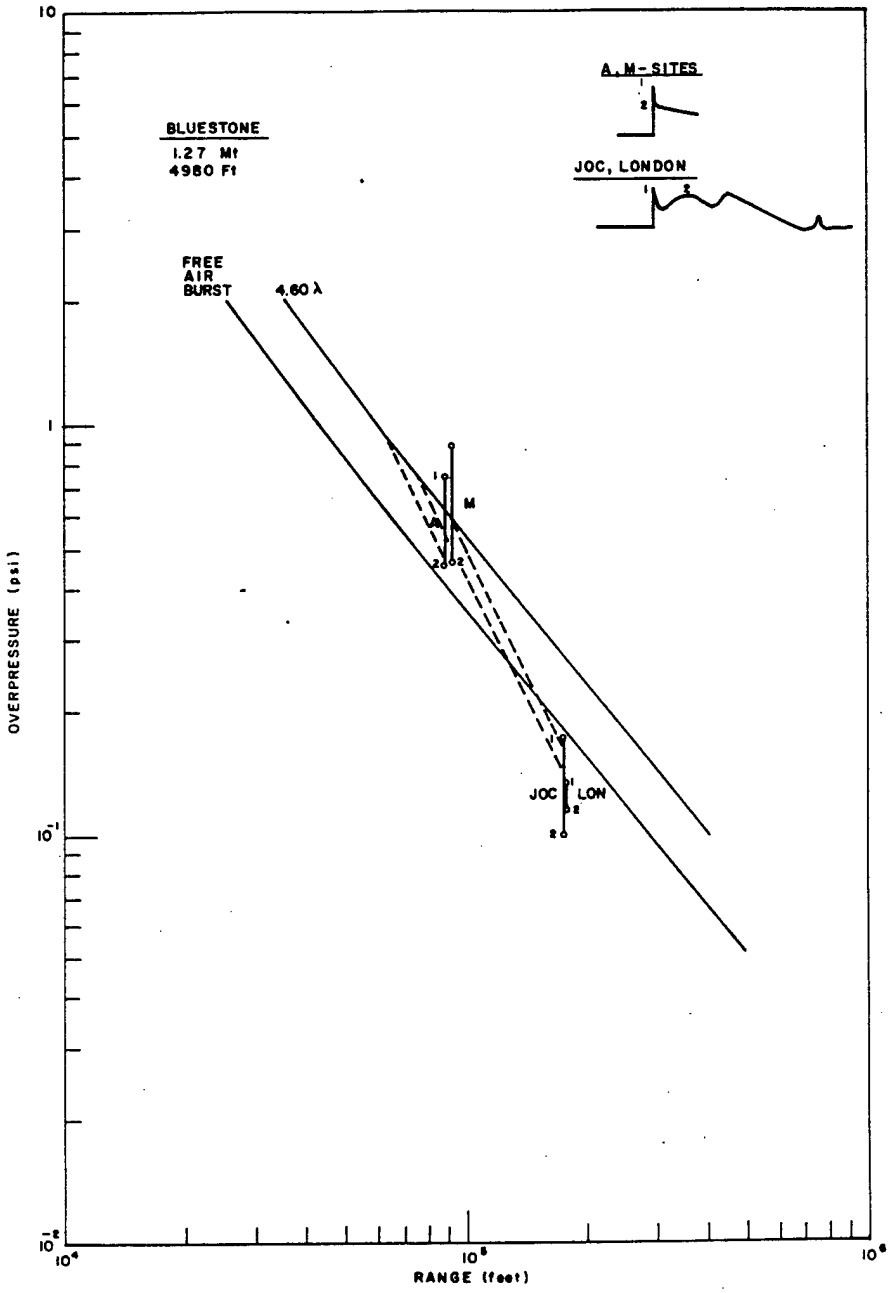

Fig. 17 Overpressure-distance calculations and measurements, Bluestone event.

3.5 Verification of Revised Predictions

Verification scatter diagrams for each of the four stations are shown in Figs. 18, 19, 20, and 21. Solid points denote predictions made from standard curves when direct ray strikes on the station were indicated by the calculated ray pattern. Open-circle points are for predictions made for diffracted waves. On JOC and London verifications, spike values are indicated when these are peak overpressures.

Standard logarithmic errors were computed to give error factors; i. e., multiplication and division of the prediction by these factors gives the range for 68 percent of the verification data. These are listed in Table 4 for each station and separately for direct ray strikes and for diffracted wave predictions, together with the various totals and subtotals. Results for Sites A and M are similar, as are results for JOC and London.

Comparison with Table 3 shows that predictions based on diffraction processes in "shadow" zones and on the standard curve where rays are computed to strike are not as accurate, over-all, as those based on the Christmas Island average curve. Better predictions, however, are made for Sites A and M by use of the ray technique. In addition, Table 4 data include all results, whereas Table 3 conclusions were formulated after deletion of "wild" data points from the calculation of averages. As a rule, the ray technique should be applicable anywhere, whereas the Christmas averages would be expected to repeat only at those same locations and under the same conditions.

TABLE 4 PREDICTION STANDARD ERROR FACTORS

	Direct		Diffracted		Total	
Station	Number of points	Error factor	Number of points	Error factor	Number of points	Error factor
Site A	6	1.497	16	1.251	22	1.330
Site M	16	1.401	8	1.210	24	1.346
JOC	2	2.635	22	1.608	24	1.705
London	2	2.331	15	1.732	17	1.806
Total	26	1.624	61	1.516	87	1.549

In summary, then, by using postshot weather, yield, and height-of-burst values, prediction standard errors were about 35 percent at A and M sites and about 75 percent at JOC and London.

Preshot predictions were, of course, less accurate, since yield was assumed (for safety) to be maximum for each device, and both height of burst and scaled height of burst were less certain. Most important, blast propagation at crosswind bearings is quite sensitive to details of wind-versus-height structure which are almost impossible to forecast. Much of postshot analysis error is undoubtedly caused by nonrepresentativeness of the furnished shot-time weather sounding which is assumed to extend over the entire propagation path. In addition, blast pressure measurements of this type usually show 10- or 20-percent instrument error and nonrepeatability, and precise verification is not possible. The over-all 55-percent standard error is at least as acceptable as are low pressure predictions for Nevada tests.[5,6] Error distribution curves for A and M sites are shown in Fig. 22 to demonstrate that verification ratios are about normally distributed, although the average observed overpressure is less than the forecast overpressure. If a 10-percent empirical reduction had been made on all predictions, however, verification standard errors would have been only slightly reduced.

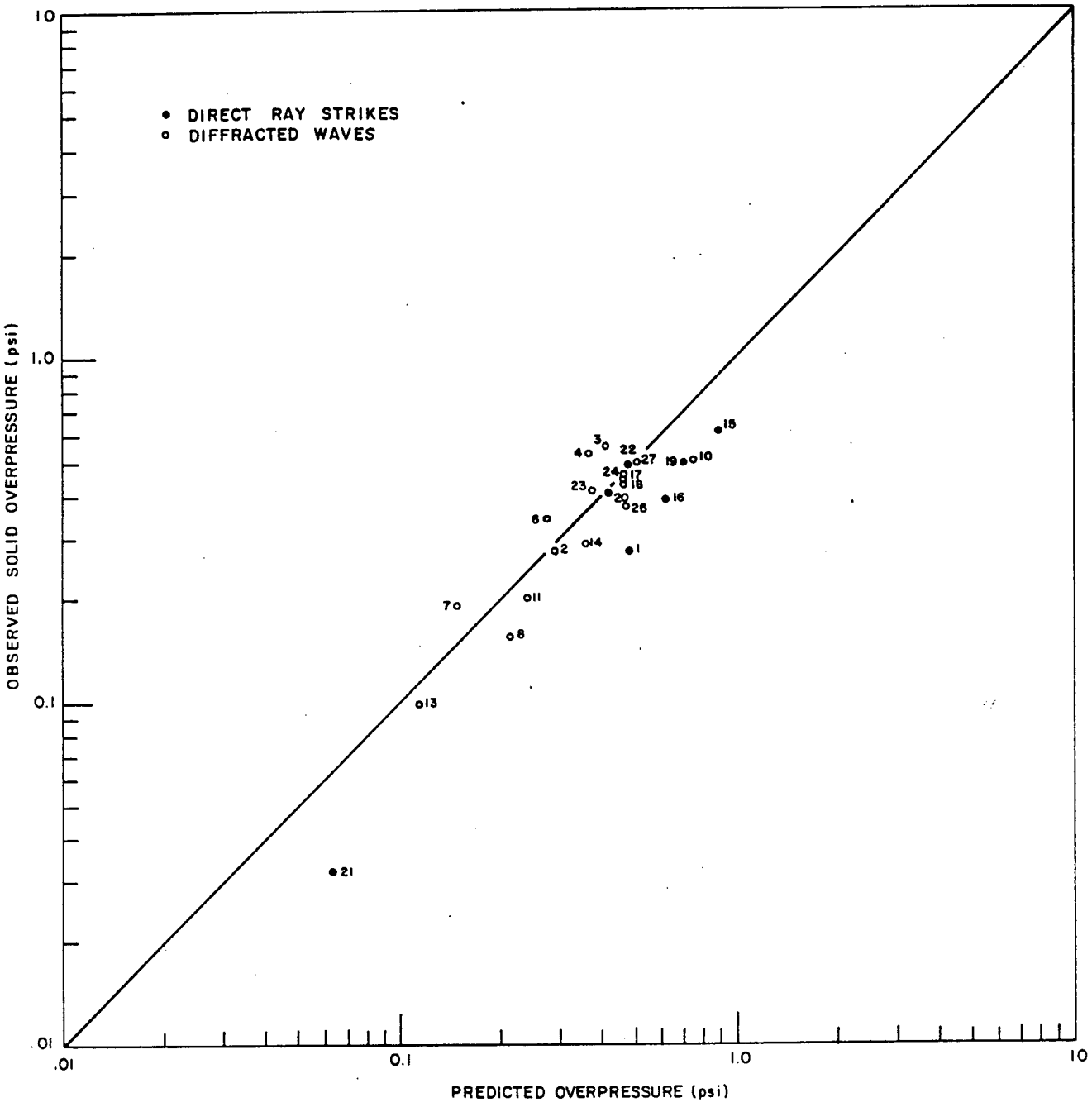

Fig. 18 Predicted versus observed overpressure scatter diagram, A site.

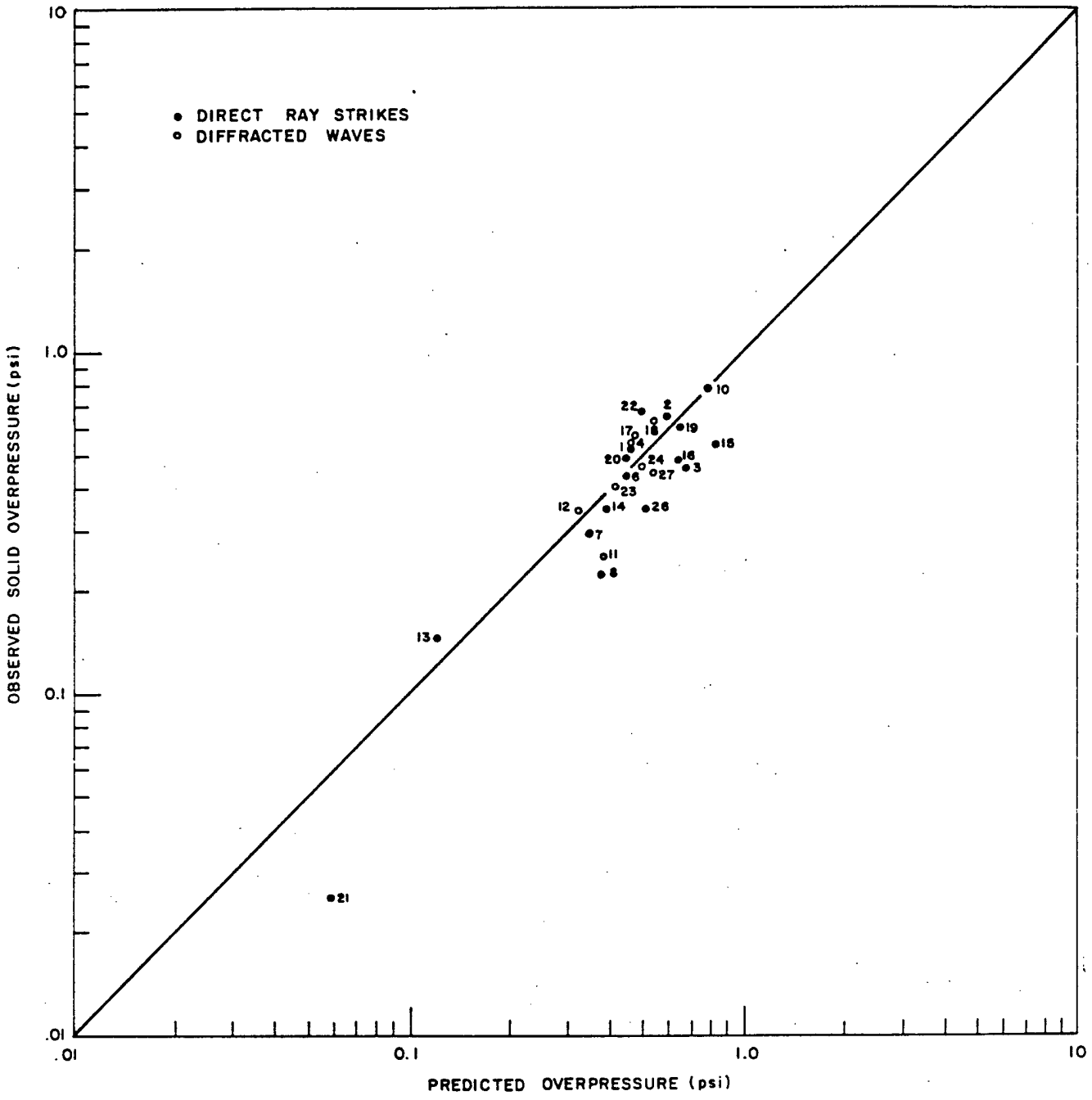

Fig. 19 Predicted versus observed overpressure scatter diagram, M site.

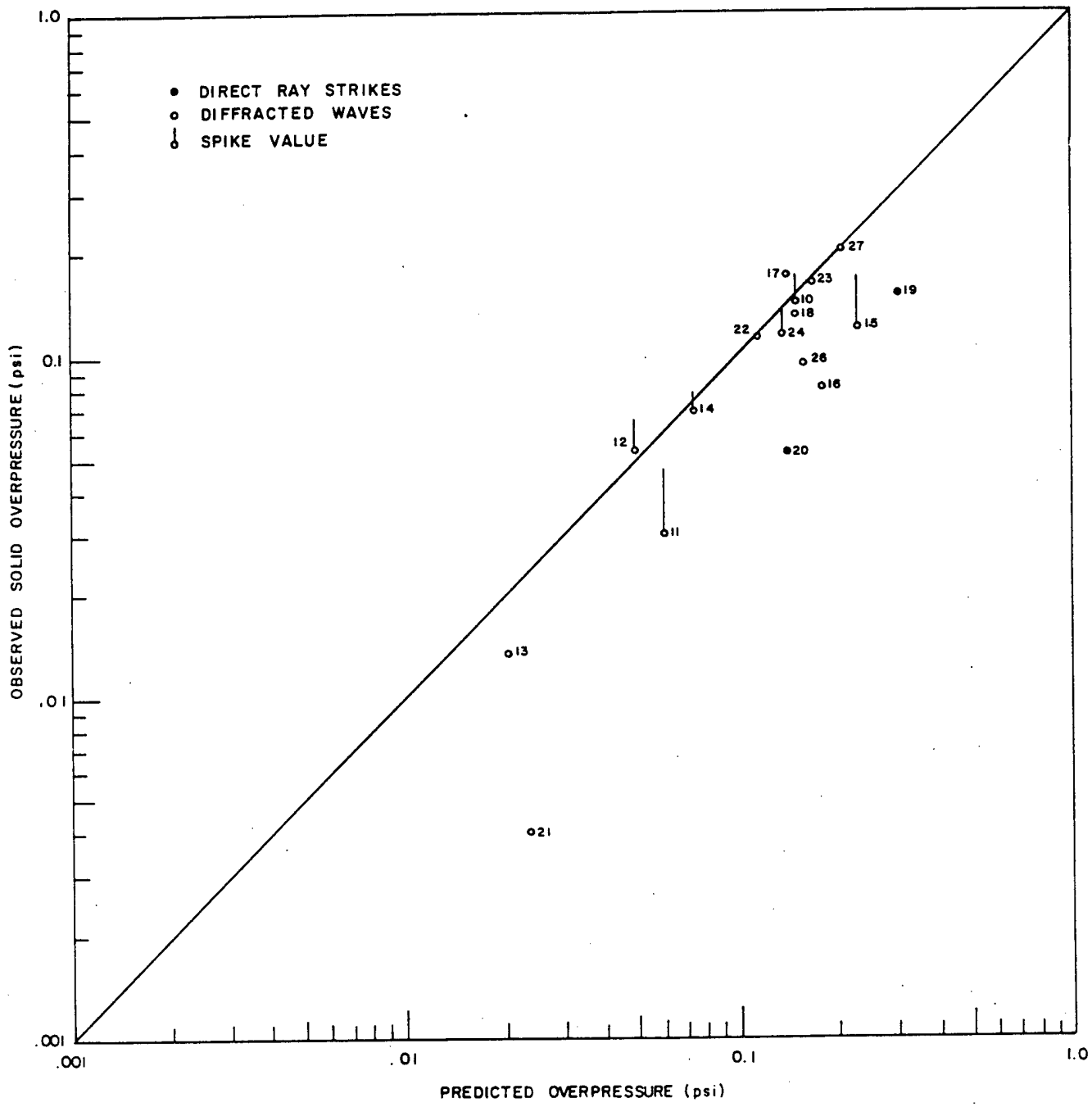

Fig. 20 Predicted versus observed overpressure scatter diagram, London.

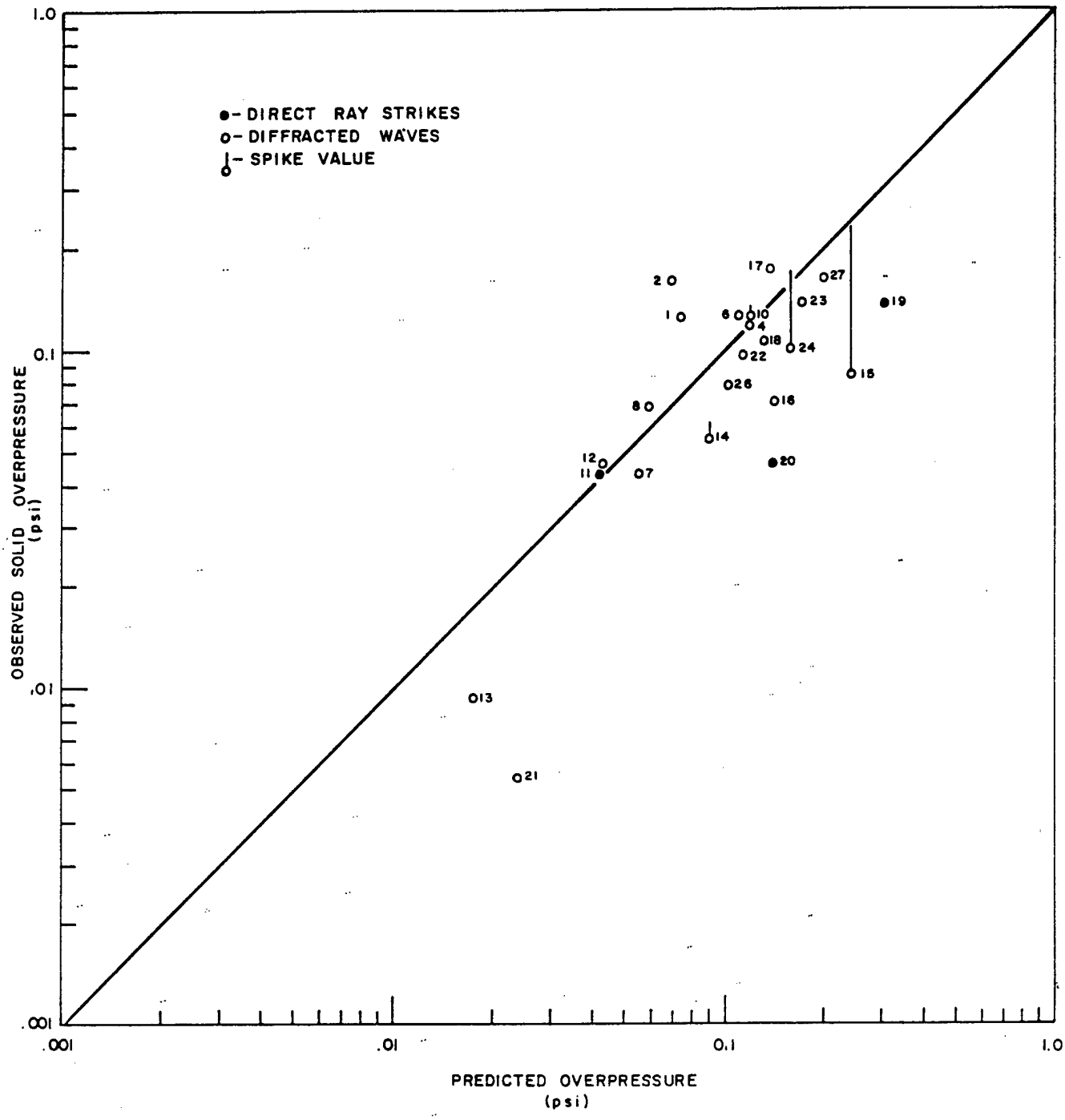

Fig. 21 Predicted versus observed overpressure scatter diagram, Joint Operations Center.

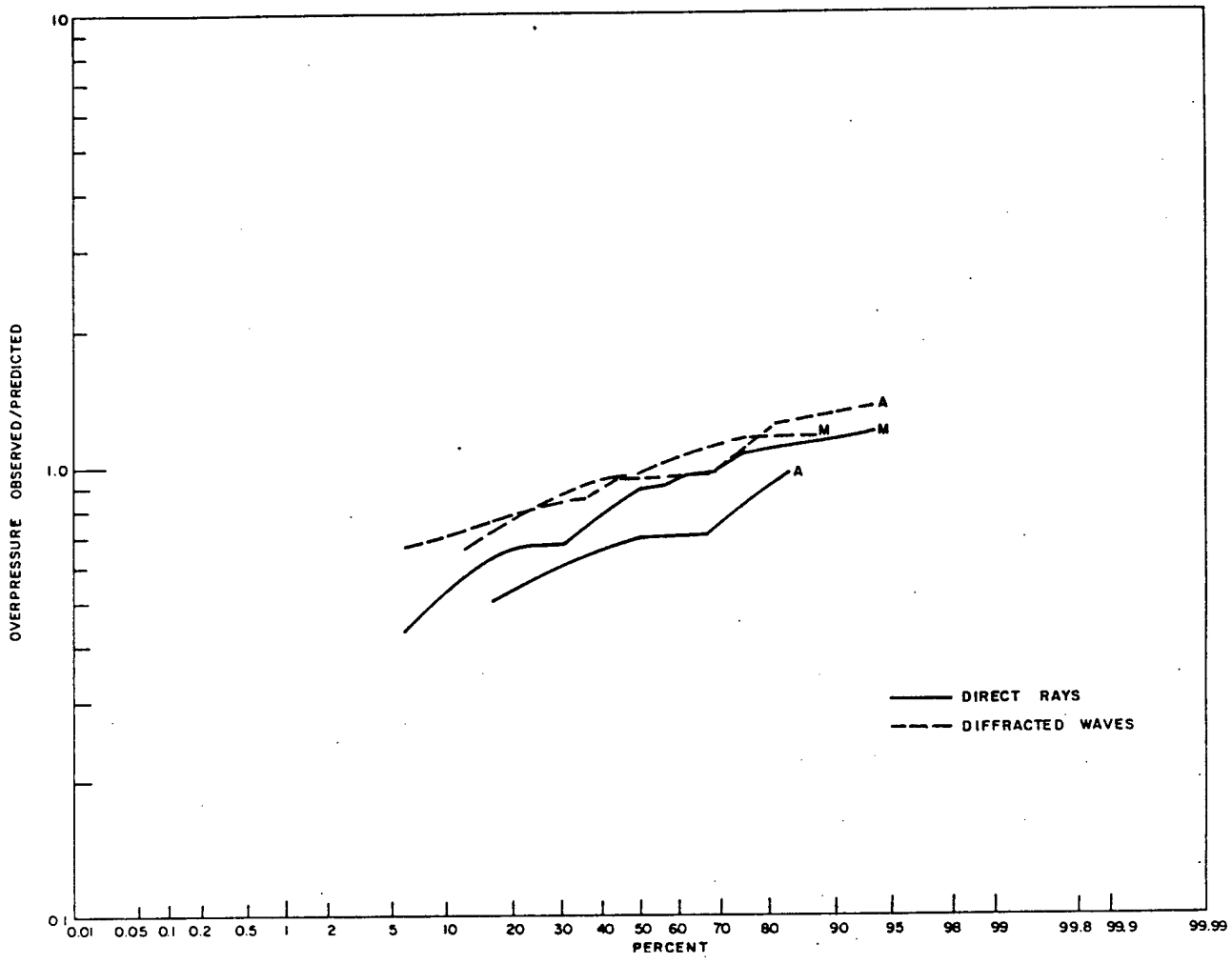

Fig. 22 Distribution of blast prediction errors.

3.6 Positive-Phase Durations

Analogous to height-of-burst overpressure relations, duration of positive blast pressure pulses is also height of burst-dependent. According to TM 23-200,[1] durations from isochrones on a 1-kt scaled height of burst versus range graph are multiplied by $W^{1/3}$ to give the duration prediction. Ambient atmospheric pressure at burst altitude was also used for scaling in accordance with conclusions from Teapot HA data,[17] although the shock moves into higher pressure air while the duration is being developed. As shown in Fig. 23, M site data from bursts below 1000 ft/(W kt Ne)$^{1/3}$ scaled height of burst demonstrate that this technique still underpredicts durations by about 30 percent. Conversely, if $W_A^{1/3}$ is used as a multiplicative factor, as employed heretofore for overpressure predictions, durations are overpredicted by about 20 percent.

Several fruitless attempts were made to derive an explanation for this discrepancy. It was found that durations continue to increase with range beyond the 10,000-foot scaled range and 0.38-second scaled duration. This has been previously found both by Cowan[18] and by Cox and Reed[5] from microbarograph measurements at long range. When found at long range, from Nevada tests, it was believed that long durations were caused by finite overpressure effects (shock velocities) in travel through the low-density high atmosphere. Such an argument is not applicable here, however, with near-sea level propagation. Extended durations were fairly uniformly observed with both spiked and unspiked pressures, which indicates that spike pressures are not the sole contributors to anomalous shock-front speeds and duration extensions.

It appears now that a revision of duration curves for height-of-burst effects may be necessary. Since duration is of prime interest only in strong dynamic pressure regions, such revision has not been attempted at this time.

3.7 Spiked Pressure Waves

The argument may be considered that pressure spikes develop on the front hillside and that an analogous ray curvature may be generated by atmospheric blast refraction away from ground. If such a conclusion were tenable, there would then be a correlation between spiking (defined as the ratio of spike overpressure to solid overpressure) and the sound velocity-height gradient which determines the ray curvature. This was tested, but it was shown instead that spiking was more prevalent when inversion conditions obtained, i.e., sound velocity increasing with height in the lowest 2000-foot layer. There is considerable scatter in the results, but a few rules-of-thumb may be derived, subject to occasional gross errors which may be caused by nonrepresentative meteorological reports. The rules, derived from Table 5, are:

1. When rays are computed to clearly miss the station and produce only a diffracted wave, there is a two-to-one probability of no spiking.
2. When a ray is computed to strike at or near the station, there is a five-to-one probability of spiking.
3. A weak indication that inversions tend to be associated with stronger spikes than are found with sound-velocity gradients is present.
4. With an inversion (>3ft/sec in 2000 feet), there is a ten-to-one probability of spiking; with nearly isovelocity or gradient structures and a direct wave, spiking probabilities are only three to one.

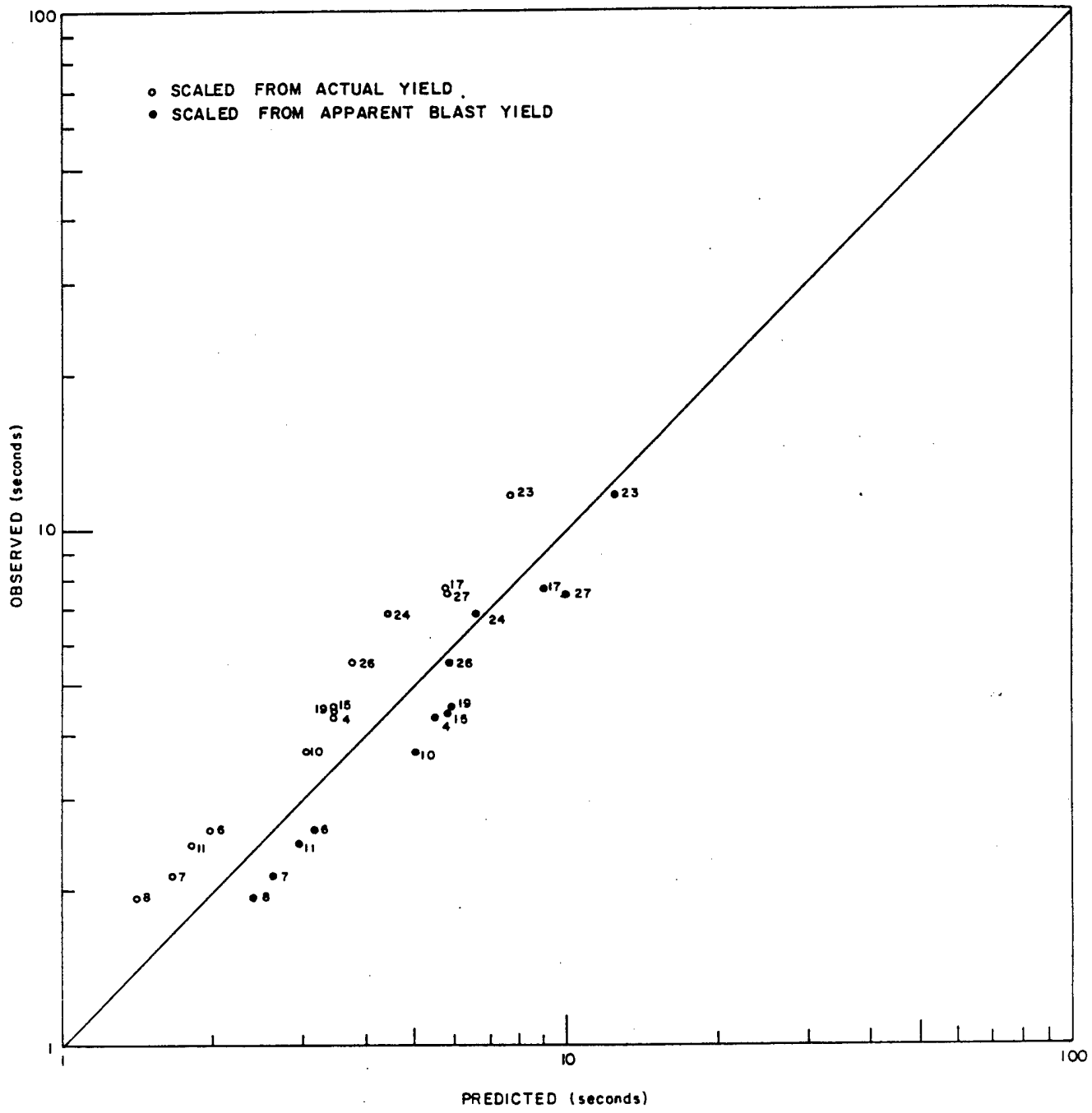

Fig. 23 Predicted versus observed positive-phase durations, M site.

Subjective observations indicated that damage and personnel response were apparently more dependent on spike or sharp pressure-rise amplitude than on long-lasting, solid overpressure. For this reason, spike predictions may prove to be of more value than the solid pressure predictions which have been of prime consideration in this report. It appears, however, that a special and more detailed weather and blast data collection program would be necessary to give further insight into spike generation.

TABLE 5 DISTRIBUTION OF SPIKED OVERPRESSURE RECORDINGS

	Spike (solid pressure)	Diffracted wave	Direct wave (dv/dz) -	0	+
No spike	≤1.0	8	3	2	0
Weak spike	1.08-1.23	1	2	3	2
Moderate spike	1.37-1.65	1	5	3	2
Strong spike	1.73-2.38	2	1	1	6

3.8 Relevant Observations

For the Bighorn event two microbarographs were operated on Johnston Island at a range of 7.145 x 10^6 feet on a bearing of 322° 32' from true north. The average recorded peak-to-peak pressure amplitude was 453 microbars, or 0.00657 psi. At this range the standard prediction line would indicate 0.0071-psi overpressure. At close-in range, standard peak-to-peak pressure is 1.35 times the overpressure, and if this ratio is assumed to be conserved at long range, the peak-to-peak prediction becomes 0.0096 psi, as shown in Fig. 24. The observed pressure was thus 0.685 times the predicted value. Prediction accuracy has not been appreciably diminished in this instance by an increase in range by a factor of 30 beyond Christmas Island measurements.

A microbarograph recording was made at JOC from the Frigate Bird event, at about 3.2 x 10^6 feet range. This shot, burst at 11,000 feet MSL, [redacted] Apparent blast yield for this height of burst [redacted] which would give a standard peak-to-peak pressure prediction of [redacted] JOC. The observed value was [redacted] which was much lower than expected downwind from ozonosphere propagation.

Neither of these two ozonosphere signals showed stronger than standard downwind propagation to long ranges as in generally experienced from Nevada tests,[6] nor do they even approach the five-times-standard amplitudes recorded upwind or crosswind at NTS from the large (62 mt) USSR test in October 1961.[19] They are, however, comparable to ozonosphere propagations recorded in the Pacific test are in past years of testing.[6]

There were no recordings made of the Dominic Swordfish event. Data from the Starfish Prime shot are included in another report on high-altitude bursts.[20]

Blast pressure recordings, made in aircraft flying in the test area, on occasion were reported to show double pulses (incident and reflected) when they were thought to be in the fused shock (Mach stem) region. This anomaly may have been caused by sound velocity-inversion effects reducing the vertical growth of the triple point. It would be of interest to compare the Air Force's airborne recording collection with computed ray patterns, as has been done in this report.

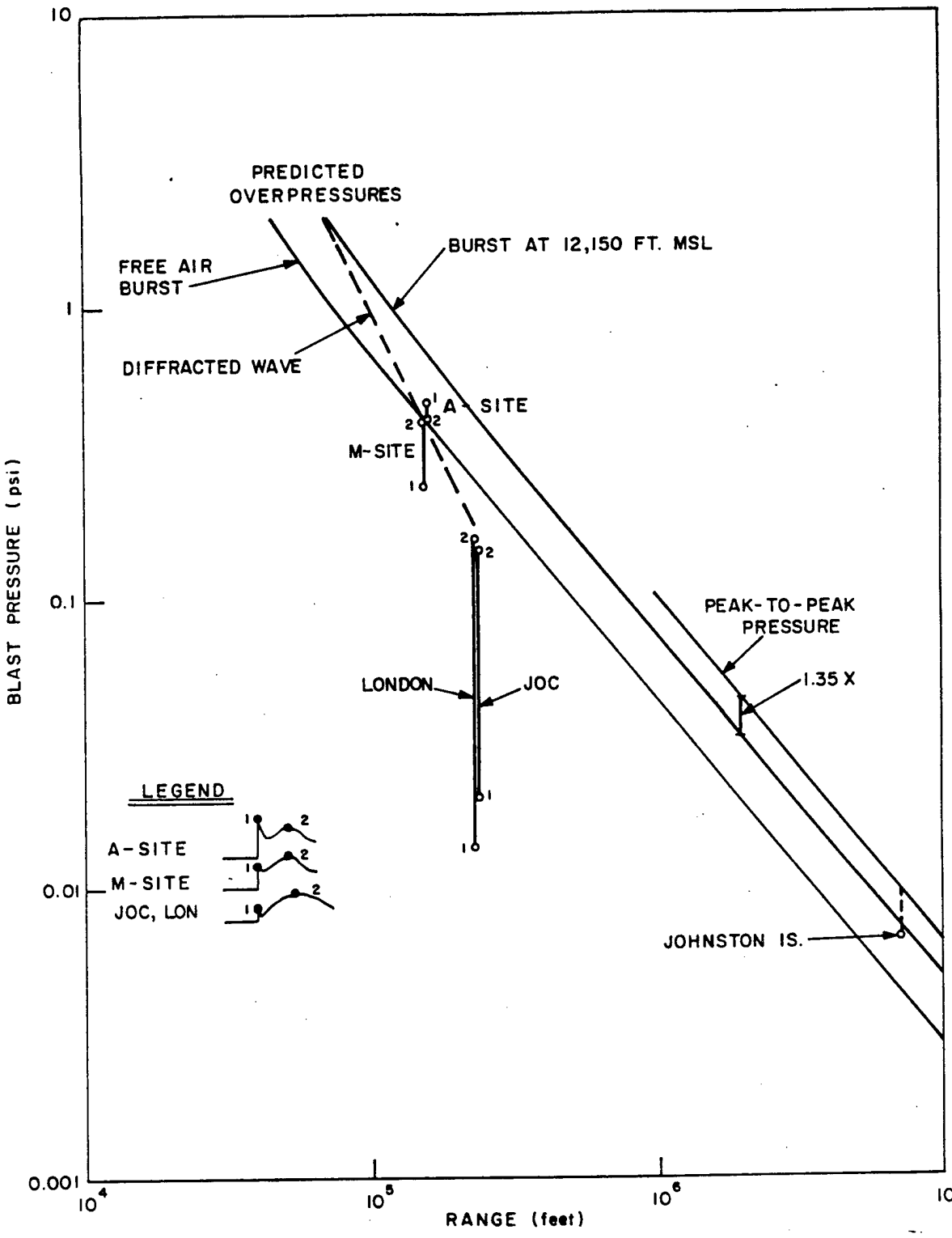

Fig. 24. Overpressure-distance calculations and measurements, Bighorn event.

4 CONCLUSIONS

Blast pressure predictions for nuclear bursts beyond the 1-psi contour require consideration of atmospheric refraction effects. For heights of burst involved in Christmas Island events, the standard scaled overpressure-distance curve may be used as far out as direct rays are calculated to land. Beyond direct ray strikes, diffractive processes feed blast energy into the "shadow" region. In this diffraction zone overpressures decay in inverse proportion to the square of the distance.

In the region of tenths of a psi, pressure spikes were frequently observed at shock arrival. Generally these did not occur with diffracted waves. Spike duration was several milliseconds, much longer than is attributable to local reflection, internal gage reactions, or electronic recording lag. Spikes may exceed double the solid overpressure value. Strongest spikes were observed when there was a sound velocity-height inversion computed for the lowest 2000 feet of atmosphere.

Blast wave positive-phase durations were generally longer than were predicted from standard curves. Durations do not seem to become constant at low overpressures; instead, they increase even faster than finite overpressure shock-speed calculations would indicate. Duration predictions for higher burst heights appear to be the most unreliable.

The standard error (logarithmic distribution) of prediction for the distance range of the A and M site instrument stations was about 35 percent; it increased to 75 percent at the range of JOC and London village. These figures take into account postshot yields and height-of-burst and weather data. Operational preshot predictions were, of course, much less accurate. Errors were caused mainly by nonrepresentative weather data observed at JOC and assumed to be constant over the 20-to-40-mile ranges of propagation. Since refracted propagation is often quite sensitive to small wind fluctuations, it would be extremely difficult and costly to attain appreciably more prediction accuracy. Future test installations should be designed to contain safely this magnitude of error.

5 RECOMMENDATIONS

Provided interest and need would justify the expense, several additional studies or measurements are suggested:

1. The spike generation mechanism should be determined. Structural responses to spikes should be measured to determine whether they are the significant light damage producers.

2. On future over-water test series of this type, measurements should be made closer to ground zero to verify height-of-burst effects and the prediction techniques derived here. Weather observations near the propagation path at mid-point should improve verifications.

3. Blast reflection factors at low incidence angles and low overpressures should be determined by experiment to find the real limits between Mach reflection, regular reflection, and grazing incidence.

REFERENCES

1. Capabilities of Atomic Weapons, S. Glasstone, ed., Departments of the Army, Navy, and Air Force, TM-23-200, November 1957. (Conf)
2. Meszaros, J. J., Retsler, R. E., and Wise, R. C., Airblast Phenomena and Instrumentation of Structures, Operation Hardtack, Project 1.7, WT-1612, Ballistic Research Laboratories, July 16, 1962. (SFRD)
3. Rollosson, G. W., Air Shock Pressure Time versus Distance, Operation Ivy, WT-602, November 1952. (SFRD)
4. Kingerg, C. N., Hoover, C. H., and Keefer, J. H., Ground Surface Air-Blast Pressure versus Distance, Operation Redwing, Project 1.1, WT-1301, Ballistic Research Laboratories, May 6, 1960. (SFRD)
5. Cox, E. F., and Reed, J. W., Long-Distance Blast Predictions, etc., General Weapons Test Report, WT-9003, Sandia Corporation, September 20, 1957. (SRD)
6. Reed, J. W., and Church, H. W., Observation and Analysis of Sounds Refracted from the Ozonosphere ..., General Weapons Test Report, WT-9005, Sandia Corporation, May 2, 1960. (SRD)
7. Division 5231, Microbarograph Evaluation Report, SC-2990(TR), Sandia Corporation, September 18, 1953.
8. Vortman, L. J., and Shreve, J. D., Jr., The Effect of Height of Explosion on Blast Parameters, SC-3858(TR), Sandia Corporation, June 20, 1956.
9. Shreve, J. D., Jr., Pressure-Distance-Height Study of 250-pound TNT Spheres, Operation Tumbler, Project 1.10, WT-520, Sandia Corporation, March 13, 1953.
10. Todd, J., Jr., and Schellenbaum, R. L., Path of Triple Point for Spherical Shocks above a Rigid Plane, SCTM 113-54(51), Sandia Corporation, July 13, 1954.
11. Stickel, M. J., A Study of Positive-Phase Impulse and Duration of Blast from Nuclear Explosions, SC-4037(TR), Sandia Corporation, January 15, 1957. (SRD)
12. Smith, L. G., Photographic Investigation of the Reflection of Plane Shocks in Air, NDRC Report A-350, Princeton University, November 1, 1945.
13. Church, H. W., Height-of-Burst Effects on Long-Range Propagated Blast Pressures, SC-4687(RR), Sandia Corporation, May 1962.
14. A Quick and Cursory Summary of the Christmas Island Portion of Operation Dominic 1962, compiled by A. L. Embry, LAMS-2757, Los Alamos Scientific Laboratory, September 1962. (SRD)
15. Broyles, C. D., IBM Problem M Curves, SCTM 268-56(51), Sandia Corporation, December 1, 1956.
16. Preliminary Report, Project Banshee Field Operations (1961 and 1962), DASA 543, Defense Atomic Support Agency, to be published.
17. Reed, J. W., et al., Ground Level Microbarograph Pressure Measurements from a High-Altitude Shot, Operation Teapot, WT-1103, Sandia Corporation, December 1955. (SRD)
18. Cowan, M., Negative-Phase Duration as a Measure of Blast Yield, SC-3170(TR), Sandia Corporation, September 1, 1953. (SRD)
19. J. W. Reed, Sandia Laboratory, to L. Machta, U.S. Weather Bureau, private communication, November 20, 1961.
20. Sandia Laboratory Staff, High Altitude Measurements, Operation Dominic, ITR-2046, Sandia Corporation, July 1963. (SRD)

DISTRIBUTION

Military Distribution Categories 2 and 12

ARMY ACTIVITIES

1 CHIEF OF R & D DA
2 AC OF S INTELLIGENCE DA
3 CHIEF OF ENGINEERS DA
4- 5 ARMY MATERIAL COMMAND
6 U S ARMY COMBAT DEVELOPMENTS COMMAND
7 U S ARMY CDC NUCLEAR GROUP
8 U S ARMY ARTILLERY BOARD
9 U S ARMY AIR DEFENSE BOARD
10 U S ARMY COMMAND AND GENERAL STAFF COLLEGE
11 U S ARMY AIR DEFENSE SCHOOL
12 U S ARMY CDC ARMOR AGENCY
13 U S ARMY CDC ARTILLERY AGENCY
14 U S ARMY AVIATION SCHOOL
15 U S ARMY CDC INFANTRY AGENCY
16 U S ARMY ORDNANCE & GUIDED MISSILE SCHOOL
17 U S ARMY CDC CBR AGENCY
18 ENGINEER SCHOOL
19 ARMED FORCES INSTITUTE OF PATH
20 ARMY MEDICAL RESEARCH LAB
21 WALTER REED ARMY INST OF RES
22 ENGINEER RESEARCH & DEV LAB
23 WATERWAYS EXPERIMENT STATION
24 PICATINNY ARSENAL
25 DIAMOND ORDNANCE FUZE LABORATORY
26- 27 BALLISTIC RESEARCH LABORATORY
28 FRANKFORD ARSENAL
29 WATERVLIET ARSENAL
30- 31 WHITE SANDS MISSILE RANGE
32 U S ARMY MOBILITY COMMAND
33 U S ARMY WEAPONS COMMAND
34 U S ARMY MUNITIONS COMMAND
35 U S ARMY ELECTRONIC PROVING GROUND
36- 37 U S ARMY CDC COMBAT SERVICE SUPPORT GROUP
38 THE RESEARCH & ANALYSIS CORP
39 WHITE SANDS SIGNAL SUPPORT AGENCY
40 U S ARMY NUCLEAR DEFENSE LABORATORY
41 U S ARMY CDC AIR DEFENSE AGENCY
42 U S ARMY COLD REGION RES & ENG LABORATORY
43 U S ARMY CORPS OF ENG NUCLEAR CRATERING
44 UNITED STATES CONTINENTAL ARMY COMMAND
45 U S ARMY CDC COMBINED ARMS GROUP

NAVY ACTIVITIES

46- 47 CHIEF OF NAVAL OPERATIONS OPO3EG
48 CHIEF OF NAVAL OPERATIONS OP-75
49 CHIEF OF NAVAL PERSONNEL
50 CHIEF OF NAVAL OPERATIONS OP-34
51- 52 CHIEF OF NAVAL OPERATIONS CODE 811
53- 54 CHIEF BUREAU OF NAVAL WEAPONS DLI-3
55- 59 CHIEF BUREAU OF NAVAL WEAPONS RAAD-221
60 CHIEF BUREAU OF MEDICINE & SURGERY CODE 74
61 CHIEF BUREAU OF SHIPS CODE 423
62 CHIEF BUREAU OF YARDS & DOCKS CODE 74
63 DIR. US NAVAL RESEARCH LAB.
64 U S NAVAL ORDNANCE LABORATORY
65 MATERIAL LABORATORY CODE 900
66 NAVY ELECTRONICS LABORATORY
67 U S NAVAL RADIOLOGICAL DEFENSE LAB
68 U S NAVAL CIVIL ENGINEERING LABORATORY
69 U S NAVAL SCHOOLS COMMAND U S NAVAL STATION
70 U S NAVAL WAR COLLEGE
71 U S NAVAL POSTGRADUATE SCHOOL
72 U S FLEET SONAR SCHOOL U S NAVAL BASE
73 U S FLEET ANTI-SUBMARINE WARFARE SCHOOL
74 U S NAVAL SCHOOL CEC OFFICERS
75 U S NAVAL DAMAGE CONTROL TNG CENTER ABC
76 AIR DEVELOPMENT SQUADRON 5 VX-5
77 NAVAL AIR MATERIAL CENTER
78 U S NAVAL AIR DEVELOPMENT CENTER
79 U S NAVAL WEAPONS EVALUATION FACILITY
80 U S NAVAL MEDICAL RESEARCH INSTITUTE
81 DAVID W TAYLOR MODEL BASIN
82 U S NAVAL ENGINEERING EXPERIMENT STATION
83 NORFOLK NAVAL SHIPYARD
84 U S PACIFIC FLEET NAVY NO 128
85 U S ATLANTIC FLEET
86 U S MARINE CORPS CODE A03H
87 FLEET MARINE FORCE ATLANTIC
88 FLEET MARINE FORCE PACIFIC
89 USMC DEVELOPMENT CENTER USMC SCHOOLS
90 USMC EDUCATIONAL CENTER USMC SCHOOLS

AIR FORCE ACTIVITIES

91- 92 HQ USAF AFTAC-TD
93 HQ USAF AFRNEA
94 HQ USAF AFXPDG
95 HQ USAF AFOWX
96- 97 HQ USAF AFXOP
98 HQ USAF AFGOA
99-103 HQ USAF AFCIN-3D1
104 AC OF S INTELLIGENCE HQ USAFE
105 RESEARCH & TECHNOLOGY DIV BOLLING AFB
106 BALLISTIC SYSTEMS DIVISION
107 HQ USAF AFMSPAA
108 TACTICAL AIR COMMAND
109 AIR DEFENSE COMMAND
110-112 AIR FORCE SYSTEMS COMMAND
113 AF COMMUNICATIONS SERVICE
114 RADC-RAALD,GRIFFISS AFB
115 PACIFIC AIR FORCES
116 SECOND AIR FORCE
117-118 AF CAMBRIDGE RESEARCH CENTER
119-121 AFWL WLL-3 KIRTLAND AFB
122-123 AIR UNIVERSITY LIBRARY
124 LOWRY TECH.TNG.CEN. TS-W
125 SCHOOL OF AVIATION MEDICINE
126-128 AERONAUTICAL SYSTEMS DIVISION
129-130 USAF PROJECT RAND
131 3535TH NAVIGATOR TRAINING WING
132 AIR TECHNICAL INTELLIGENCE CENTER
133 HQ USAF AFORQ

OTHER DEPARTMENT OF DEFENSE ACTIVITIES

134 DIRECTOR OF DEFENSE RESEARCH AND ENGINEERING
135 ASST TO THE SECRETARY OF DEFENSE ATOMIC ENERGY
136 ADVANCE RESEARCH PROJECT AGENCY
137 WEAPONS SYSTEM EVALUATION GROUP
138 ASST SECRETARY OF DEFENSE INSTALLATION & LOGISTICS
139-142 DEFENSE ATOMIC SUPPORT AGENCY
143 FIELD COMMAND DASA
144 FIELD COMMAND DASA FCTG
145-146 FIELD COMMAND DASA FCWT
147-148 DEFENSE INTELLIGENCE AGENCY
149 ARMED SERVICES EXPLOSIVES SAFETY BOARD
150 JOINT TASK FORCE-8
151 COMMANDER-IN-CHIEF EUCOM
152 COMMANDER-IN-CHIEF PACIFIC
153 COMMANDER-IN-CHIEF ATLANTIC FLEET
154 STRATEGIC AIR COMMAND
155 CINCONAD
156-158 ASST SECRETARY OF DEFENSE CIVIL DEFENSE

SPECIAL DISTRIBUTION

159 AFCRL,TERRESTIAL SCIENTIFIC LAB-E.ILIFF
160 SYLVANIA ELECTRONIC DEF.LAB.-HARDING
161 US ARMY BALLISTIC RESEARCH LAB-MESZAROS
162 US NAVAL ORDNANCE LABS.-RUDLIN
163 NATIONAL CENTER FOR ATMOSPHERIC RES.-REX
164 US WEATHER BUREAU RES.STATION-ALLEN
165 UNIV.OF CALIF. LAWRENCE RAD. LAB-SHELTON
166 LOS ALAMOS SCIENTIFIC LAB.-STOPINSKI
167 US ARMY ELEC.RES.&DEV.ACTIVITY-WEBB
168 US AIR FORCE AERO.SYSTEMS DIV.-BACHMAN

ATOMIC ENERGY COMMISSION ACTIVITIES

169-171 AEC WASHINGTON TECH LIBRARY
172-173 LOS ALAMOS SCIENTIFIC LAB
174-190 SANDIA CORPORATION
191-200 LAWRENCE RADIATION LAB LIVERMORE
201-204 NEVADA OPERATIONS OFFICE,LAS VEGAS
205 DTIE OAK RIDGE,MASTER
206-235 DTIE OAK RIDGE SURPLUS